

From the Klinik für Urologie und Kinderurologie
(Director: Prof. Dr. Klaus-Peter Jünemann)
at the University Medical Center Schleswig-Holstein, Campus Kiel
at Christian-Albrechts-Universität zu Kiel - Kiel University

**Internal Landmarks of the prostate in transrectal ultrasound as basis for
long-term monitoring and targeted biopsy: an observational study**

Dissertation
to acquire the doctoral degree (Dr. med.)
at the Faculty of Medicine
at Christian-Albrechts-Universität zu Kiel - Kiel University

presented by
Yanqi Xie
from **Hangzhou, Zhejiang, China**

Kiel 2020

1st Reviewer: Prof. Dr. Tillmann Loch

2nd Reviewer: Prof. Dr. Jochen Cremer

Date of oral examination: 17.01.2022

Approved for printing, Kiel, 01.09.2021

Signed: Prof. Dr. Franziska Theilig

(Chairperson of the Examination Committee)

Table of contents

Table of contents	I
Abbreviations	III
1. Introduction	1
2. Materials and methods	8
2.1. Landmarks validation in vitro	8
2.2. Landmarks study in vivo	10
2.2.1. Landmarks in single AI-US-CT session	10
2.2.2. Landmarks in multiple AI-US-CT sessions (Trend Monitoring)	12
2.2.2.1. Study population	12
2.2.2.2. The SOP of AI-US-CT examination	13
2.2.2.3. Data collection and statistical calculation	25
3. Results	27
3.1. Landmarks validation in vitro	27
3.2. Landmarks study in vivo	28
3.2.1. Landmarks in single AI-US-CT session	28
3.2.2. Landmarks in multiple AI-US-CT sessions (Trend Monitoring)	28
3.2.2.1. General clinical characteristics	29
3.2.2.2. Characteristics of landmarks	33
3.2.2.3. Characteristics of targeted biopsies	36
4. Discussion	40
4.1. Study objectives	40
4.1.1. Current dilemmas and challenges in urologic imaging	40
4.1.2. Initial questions of current study	41
4.2. Study findings	42
4.2.1. Functionality of Internal Landmarks (the first question)	42
4.2.2. Characteristic Internal Landmarks (the second question)	44
4.3. Internal Fusion vs. External Fusion	46
4.4. Study limitations and future developments	48

5. Conclusion	50
6. Bibliography	52
7. Appendices	59
7.1. Figure and table index	59
7.2. Permissions of reusing published figures	60
7.3. Publications	60
8. Acknowledgements	62
9. Curriculum Vitae	63

Abbreviations

AI artificial intelligence

AI-US-CT ultrasound computed tomography with artificial intelligence

ANNA/C-TRUS artificial neural network analysis/computerized transrectal ultrasound

ASR age-standardized rates

BPH benign prostatic hyperplasia

DRE digital rectal examination

f/t PSA free/total PSA ratio

GS Gleason Score

IGRT image-guided radiotherapy

IPSS International Prostate Symptom Score

ISUP International Society of Urological Pathology

LUTS lower urinary tract symptoms

mpMRI multiparametric magnetic resonance imaging

PAE prostate adenoma enucleation

PCa Prostate cancer

PI-RADS Prostate Imaging Reporting and Data System

PSA prostate-specific antigen

PSAD PSA density

PSAV PSA velocity

PZ peripheral zone

RCT randomized controlled trial

ROI region of interest

RP radical prostatectomy

SOP standard operating procedure

TRUS transrectal ultrasound

TURP transurethral resection of the prostate

US ultrasound

1. INTRODUCTION

The prostate is a compound tubulo-alveolar endocrine and exocrine gland, normally chestnut-sized, in the male reproductive system. The most important function of the prostate is to produce and secrete a slightly alkaline fluid that constitutes approximately 30% of the ejaculatory volume [1]. The smallest structural components of the gland, the prostatic acini, are surrounded by a basement membrane which separates the secretory epithelial cells from the surrounding structures. Abnormal proliferation of cells through the basement membrane leads to prostate cancer (PCa) [2].

PCa is the second most commonly diagnosed cancer and the fifth (the second in Germany) leading cause of cancer mortality in men [3]. In 2012 alone, an estimated number of 1.1 million men were diagnosed with PCa globally, thus representing a substantial public health burden [4]. The incidence of PCa diagnosis varies widely between different geographical areas, being low in Eastern and South-Central Asia (age-standardized rates [ASR] per 100,000 of 10.5 and 4.5, respectively), while being high in Australia/New Zealand and Northern America (ASRs 111.6 and 97.2), and in Western and Northern Europe (ASRs 94.9 and 85), mainly due to the aging population and the application of prostate-specific antigen (PSA) testing [4, 5].

Early stage PCa is generally asymptomatic, and the suspicion is often raised on the basis of serum PSA level and/or digital rectal examination (DRE) and/or prostate imaging [6]. However, it has always been challenging to determine a reliable serum PSA cutoff that can indicate the presence of PCa, because serum PSA is an organ-specific biomarker rather than being tumor-specific, which may also be elevated in prostatitis, benign prostatic hyperplasia (BPH) and other non-malignant conditions [7]. Similarly, neither the other two predictors (abnormal lumps by DRE and/or suspicious imaging) alone can confirm the early diagnosis [8].

At present, the only definitive approach to confirm or rule out PCa before prostatic operations (e.g. radical prostatectomy [RP], transurethral resection of the prostate [TURP]) depends on histopathological verification of samples in prostate biopsy cores, which means removal of prostate tissues from several pre-determined sites within the gland utilizing a spring-driven biopsy gun with a thin, hollow needle. Current guidelines recommend ultrasound (US) guided ten to twelve cores systematic biopsy via transrectal or transperineal approach as the standard of care [6, 9, 10]. However, random systematic biopsies have nothing to do with specific targeting on cancerous tissues. Studies have indicated that initial biopsies by these non-targeted methods fail to detect PCa in 21–47% of patients and 20–60% of morphologically suspicious US lesions prove to be benign [11–14]. The interpretation of the TRUS images is subjective and varies dramatically by examiners' experience. These disadvantages of systematic biopsy necessitate the further development of targeted biopsies guided by different imaging modalities.

Due to technology developments, there is nowadays more information available for specific diagnosis interpretation of PCa. Advances have been made in multiparametric magnetic resonance imaging (mpMRI) and US based technologies [15–18]. To overcome the difficulties of cognitive correlation of cross-sectional suspicious areas, fusion biopsies were facilitated to target lesions, which are visible on an external imaging modality (e.g. mpMRI), under US guidance. However, controversy still remains on the accuracy of true targeting lesions which is susceptible to factors such as prostate displacements occurred in the time-consuming fusion process and variation of mpMRI results due to inter-reader subjective interpretation. One modern innovative approach that utilizes direct targeting of the transrectal ultrasound (TRUS) detected lesions is artificial neural network analysis/computerized TRUS (ANNA/C-TRUS) [19] and it has opened a new way of objective image interpretation of the prostate with guideline recommended TRUS biopsy method. In *Campbell-Walsh Urology 10th Edition* it is highlighted:

Artificial neural networks are another potential way to enhance TRUS images and identify malignant foci. Investigational automated image analysis, including pattern recognition and artificial neural networks applied to TRUS images, may successfully identify lesions that cannot be seen by the human eye.

This sophisticated artificial intelligence (AI) algorithm was established upon a large series of accurately correlated fusion between TRUS imaging and pathological findings on RP specimens [20]. Preoperative gray-scale TRUS transverse images were obtained (Fig. 1a) and digitalized to generate subvisual image information (Fig. 2). Postoperative pathologically review-and-marked whole-mount sections were also scanned as digital files (Fig. 1b), virtually overlaid on the corresponding TRUS images by utilizing computerized “transparent projection”. All sectioned benign regions, low-grade (Gleason grade 1–3) and high-grade (Gleason grade 4–5) cancers on pathology were correlated with their own characteristics of US signal, disregarding echogenicity (Fig. 1c). The computer-generated, pathologically confirmed numeric descriptor data were then used to train ANNA (Fig. 2). Set-up of artificial neural network enabled ANNA/C-TRUS to detect and mark cancer-suspicious areas upon the conventional TRUS image (Fig. 1d). Over the last decade, ANNA/C-TRUS was utilized for targeted biopsy in multiple hospitals in Germany, France, Sweden, Norway, Austria, Poland and China, and has been a routine way to guide prostate biopsy for patients and also applied as ultrasound computed tomography with AI (AI-US-CT) in everyday clinical practice in our institution (Department of Urology, Diakonissen Hospital, Flensburg) [21–24].

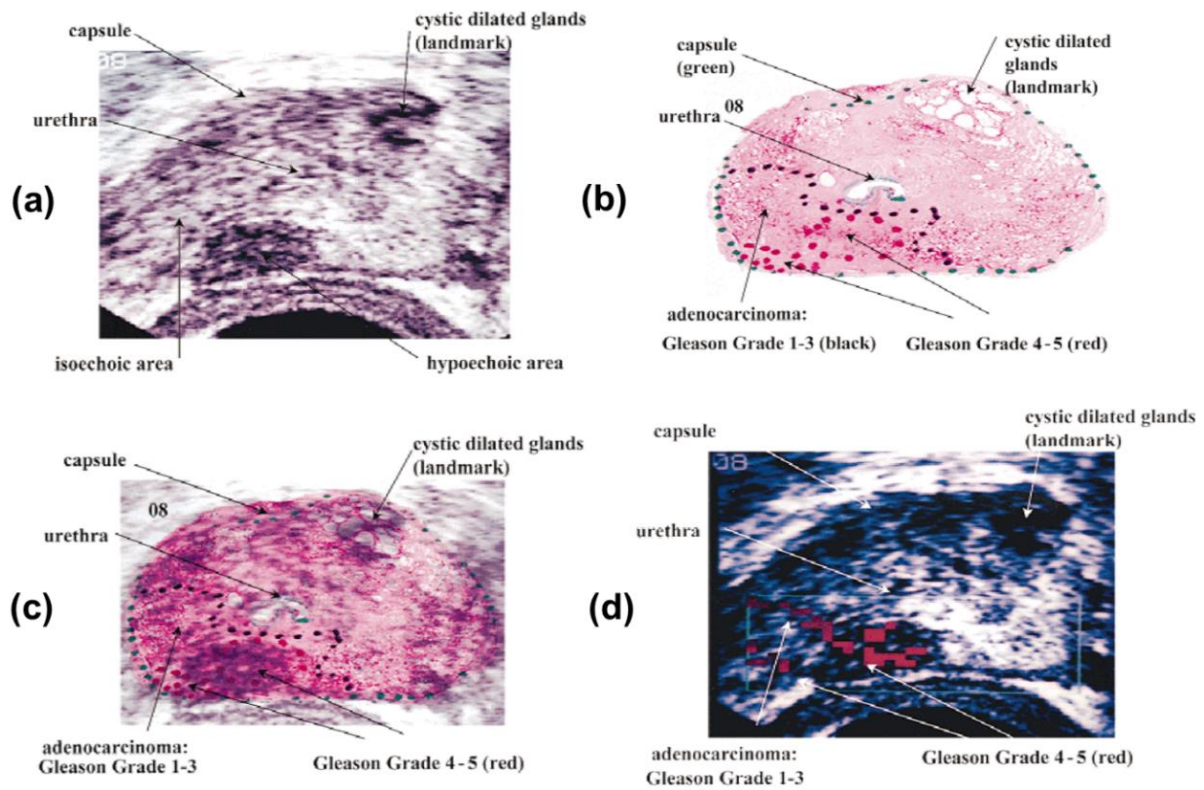


Fig. 1 Depiction of ANNA/C-TRUS (Adopted from [20] with the permission of the publisher: license number 4766010750152). (a) Transverse TRUS image of the prostate. (b) Pathologic whole-mount transverse section of the prostate (same cross-section as Fig. 1a). (c) Transparent projection of pathology slice and TRUS image. (d) ANNA result for image shown in Fig. 1a. Red boxes mark cancer-suspicious areas for targeted biopsy.

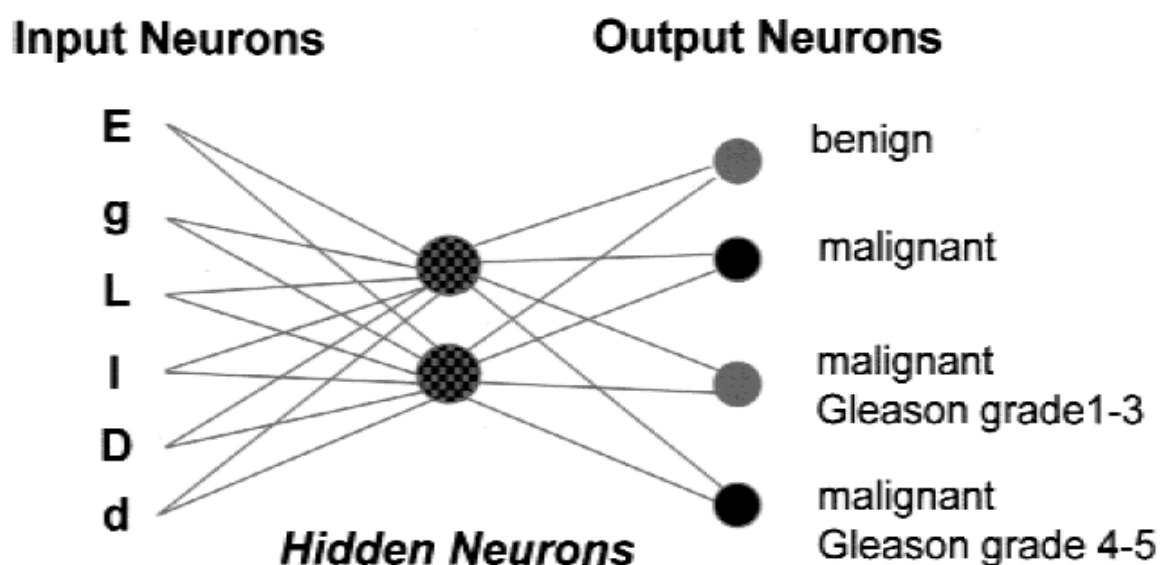


Fig. 2 Diagram of the artificial neural network used for ANNA (Adopted from [20] with the permission of the publisher: license number 4766010750152). The input neurons are weighted by the hidden network neurons so that the best output results are generated.

To translate any image-based biopsy modality into application, it needs to be ascertained that the regions marked as cancer-suspicious truly represent the corresponding areas of the prostate. Furthermore, to reliably implement “Trend Monitoring”, which means monitor changes in prostate tissue over time, it is essential to identify the same cross-sections at different time intervals. However, continuous assessment of a certain cross-section of the prostate and re-location of the same suspicious lesions in a longitudinal observation constitute the main challenge during the monitoring as well as the fusion process for targeted biopsies with other imaging techniques, these dilemmas may cause direct influence on predicting outcomes and deciding re-biopsy or treatment switching timing for patients under active surveillance [25].

In this approach the question was tried to be answered: is there a practical solution for the aforementioned difficulties, based on the existing medical facilities and methods? Fiducial

markers surgically implanted in prostate (Fig. 3) prior to image-guided radiotherapy (IGRT) for PCa are an excellent surrogate for prostate position, enabling precise treatment delivery and minimizing the radiation dose to the surrounding organs [26]. Applications of these artificial landmarks as a location method inspired us to put forward the hypothesis: natural findings in the prostate such as e.g. calcifications or cysts, which are TRUS-identifiable, could also possibly be taken as the anchor points to facilitate exact imaging correlation and target biopsies precisely. As shown previously in figure 1c, during the development process of ANNA/C-TRUS, cystic dilated glands or other distinguishing marks were utilized in “transparent projection” for confirming lesion location and accurate pathology/TRUS fusion (“Internal Fusion”), this “landmark technique” allowing for circa 2 mm accuracy in correlation [20]. But how would these landmarks within the prostate gland, termed as “Internal Landmarks”, perform in long-term clinical practices, even up to ten years?



Fig. 3 TRUS image of fiducial markers (“gold seeds”) utilized in IGRT for PCa treatment.

Therefore, the objectives of the current study were:

- (1) verify the feasibility of Internal Landmarks in assistance for Trend Monitoring and targeted biopsy by ANNA/C-TRUS through an observation of the routine clinical practice in our institution;
- (2) find out which specific kind of Internal Landmarks are the most representative to be applied;
- (3) formally document the methodology of Internal Fusion and the standard operating procedure (SOP) of AI-US-CT for urologists.

2. MATERIALS AND METHODS

2.1. Landmarks validation in vitro

Before the study in vivo, the functionality of Internal Landmarks for TRUS images correlation was verified in a simulation setting in vitro. The purpose of this preliminary verification was also to further familiarize the operators with the imaging approaches which would later be carried out. An US phantom (CIRS Model 053, Computerized Imaging Reference Systems, Inc, USA) was utilized to simulate the real prostate and relevant anatomy (Fig. 4). Firstly, one cross-section of the phantom including fixed size artificial anchor points (Internal Landmarks) was selected and corresponding TRUS image was obtained on the first US equipment (Pro Focus 2202 system, 8808 transducer, B-K Medical, Denmark) (Fig. 5a). Subsequently, two urologists in our institution tried to re-identify the previously viewed cross-section according to transversal and longitudinal correlation of the immobile Internal Landmarks, respectively on other three different models of US instruments, at different times (Fig. 5b-d):

- (1) Viking 2400 system, 8808 transducer, B-K Medical, Denmark
- (2) Pro Focus 2202 system, 8818 transducer, B-K Medical, Denmark
- (3) bk5000 system, E14C4t transducer, B-K Medical, Denmark

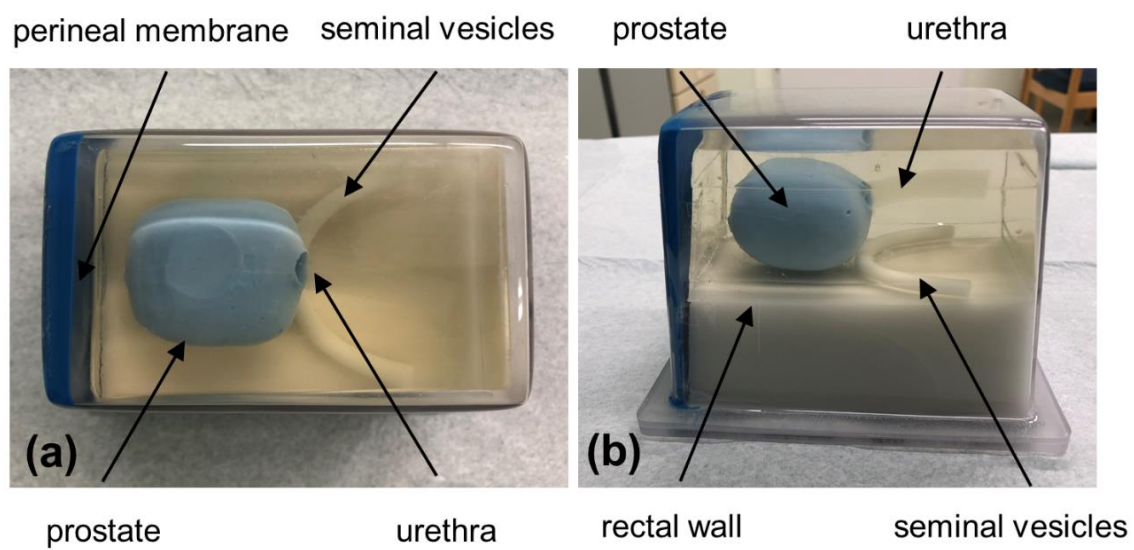


Fig. 4 Ultrasound prostate phantom utilized for the preliminary verification in vitro. (a) Top view. (b) Side view.

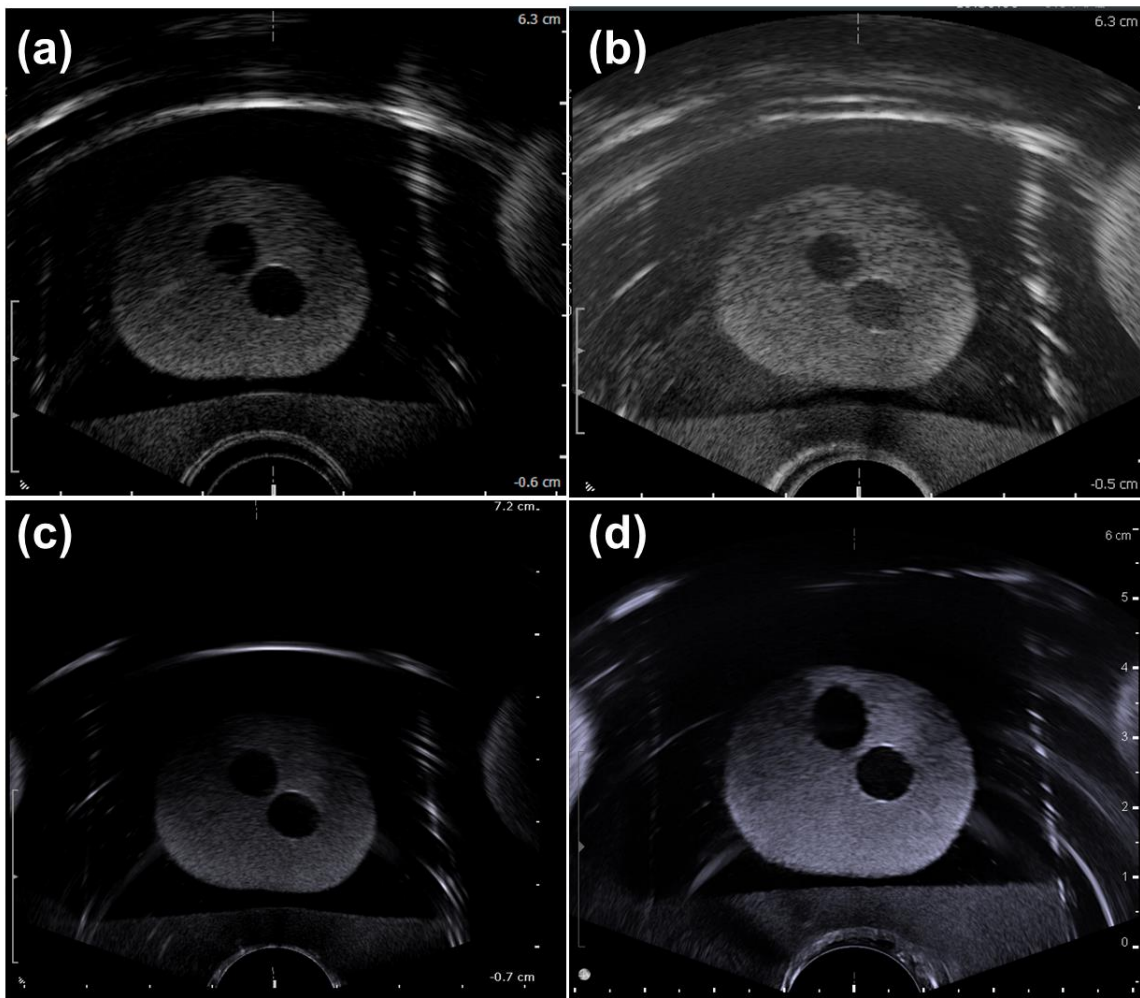


Fig. 5 Validation of Internal Landmarks (bubbles) in prostate phantom by different ultrasound equipment with respective parameter settings. (a) Pro Focus 2202, transducer 8808 at 8 MHz. (b) Viking 2400, transducer 8808 at 8 MHz. (c) Pro Focus 2202, transducer 8818 at 12 MHz. (d) bk5000, transducer E14C4t at 9 MHz.

Finally, the number of total TRUS images and the number of TRUS images which could be re-identified on the basis of Internal Landmarks were recorded for calculation of the correlation rate.

2.2. Landmarks study in vivo

2.2.1. Landmarks in single AI-US-CT session

When inspecting through the prostate under TRUS, distinguishing findings such as calcifications, cysts, and zonal anatomy, were naturally considered to be ideal candidates for Internal Landmarks. These anchor points determined in the first AI-US-CT session are essential for TRUS images correlation in the following sessions in future, thus it needs firstly to be verified that they were reproducible to be identified in a single session. The operator chose a specific cross-section of the prostate including Internal Landmarks to generate corresponding TRUS image. After repositioning the transducer quickly, such as rotating, angling, or cephalad and caudally moving, he attempted to obtain TRUS images as identical as possible to the initial one, as a proof of successful re-identification of the initial Internal Landmarks (Fig. 6a). Additionally, only for validation at the beginning, two more operators tried to respectively duplicate this procedure in the same session (Fig. 6b, c). Informed consent was obtained prior to the examination.

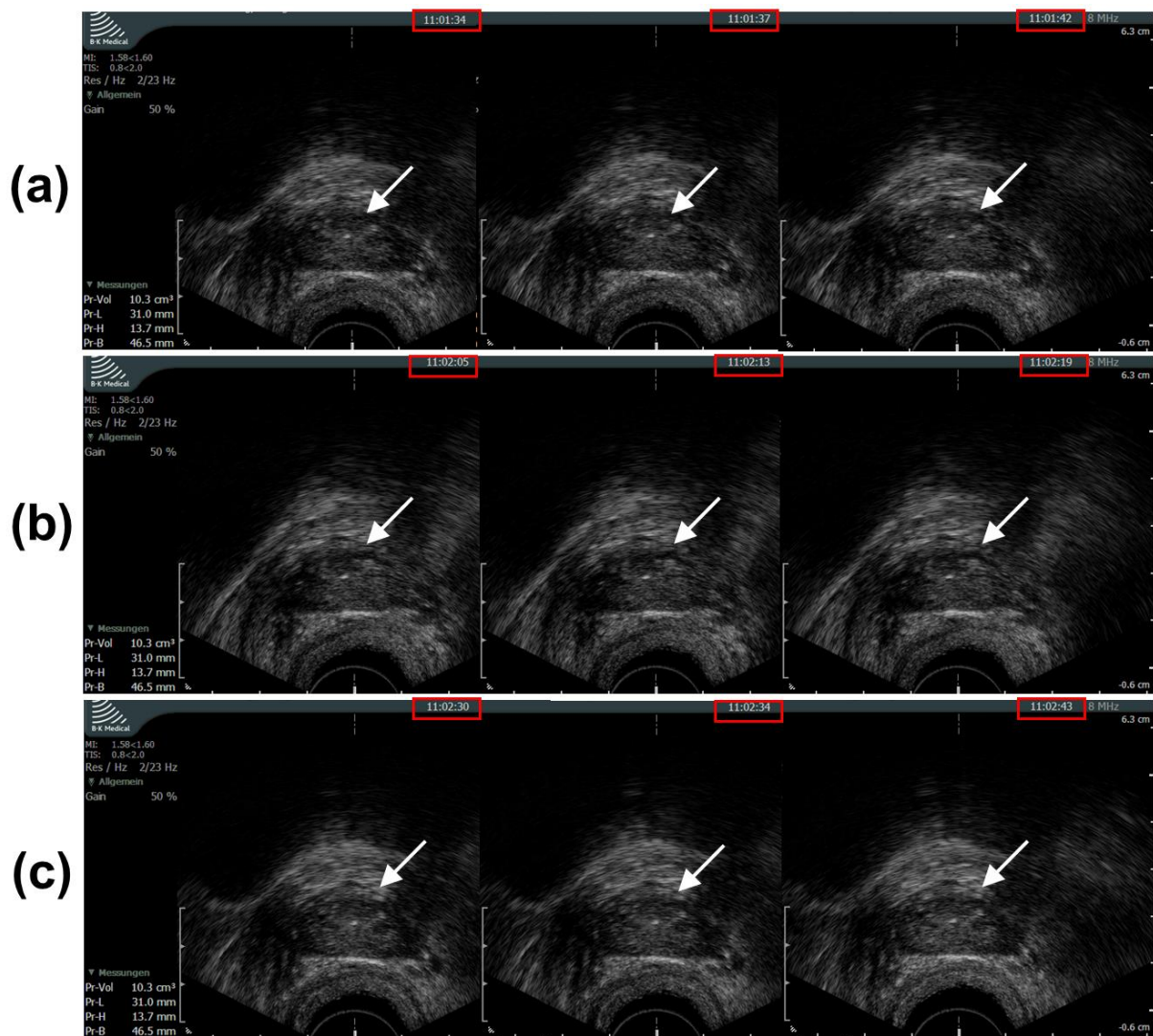


Fig. 6 TRUS images of a cross-section 5 mm from the apex of the prostate (Pro Focus 2202 system, 8808 transducer, B-K Medical, Denmark). This cross-section was re-identified, even after repositioning the transducer, by correlating to Internal Landmarks on the scale of millimeter (*white arrows*). The visually identical TRUS images were obtained within one single AI-US-CT session, but respectively by three operators at different times (*red boxes*). (a) By doctor 1. (b) By doctor 2. (c) By doctor 3.

2.2.2. Landmarks in multiple AI-US-CT sessions (Trend Monitoring)

2.2.2.1. Study population

From January 2017 to May 2018, data were collected from patients who came for prostate diagnostic consultation in our institution.

The inclusion criteria for this study were:

- (1) Patients who had undergone at least one AI-US-CT session prior to the inclusion, with the corresponding digitally documented serial TRUS images of the prostate which could be retrospectively viewed;
- (2) Good imaging quality of the prostate;
- (3) Patients being well informed about this study and gave the informed consent of their TRUS images and other medical data being processed for storage, transmission, analysis, review and other relevant purposes.

The exclusion criteria for this study were:

- (1) Patients who carried an indwelling catheter or metal intraprostatic stent when undergoing the AI-US-CT examination.
- (2) Patients with incomplete essential data information.

Trend Monitoring was stopped only when PCa was diagnosed and RP was performed, or when patients choose to stop the follow-up procedure.

2.2.2.2. The SOP of AI-US-CT examination

In our institution, ANNA/C-TRUS has been utilized since 2004 for imaging of multiple cross-sections in the prostate as a routine examination, that is, to generate a series of original and AI algorithms analyzed consecutive transverse TRUS images. Therefore, this technique was termed as “artificial intelligent ultrasound computed tomography” (AI-US-CT) [24].

(1) Ultrasound device

TRUS imaging was performed with a Pro Focus 2202 US instrument utilizing a model 8808 biplane transducer at 8 (5–10) MHz frequency (B-K Medical, Denmark). Standard setup

parameters (Prostate 8.0) were employed (MI $1.58 < 1.60$, TIS $0.8 < 2.0$, Res/Hz 2/23 Hz, gain 50%, dynamic range 74 dB, harmonic off, persist 5, edge 2, line density 3, multibeam 1, noise reject 5, gray-scale 8). The gain can be altered to achieve the optimal brightness setting, which results in a medium-gray image of the normal peripheral zone (PZ). This gray tone serves as the reference point for judging lesions as hypoechoic, hyperechoic, isoechoic, or anechoic (darker, lighter than or similar to the normal PZ, or completely black). A water balloon standoff (usually filled with 5–20 mL of degassed water while scanning) mounted on the end of the probe was applied to improve contact and field of view during transrectal imaging of the prostate (Fig. 7). By varying the amount of water in the balloon, it is possible to optimize the transducer's focal zone orientation in the tissue.

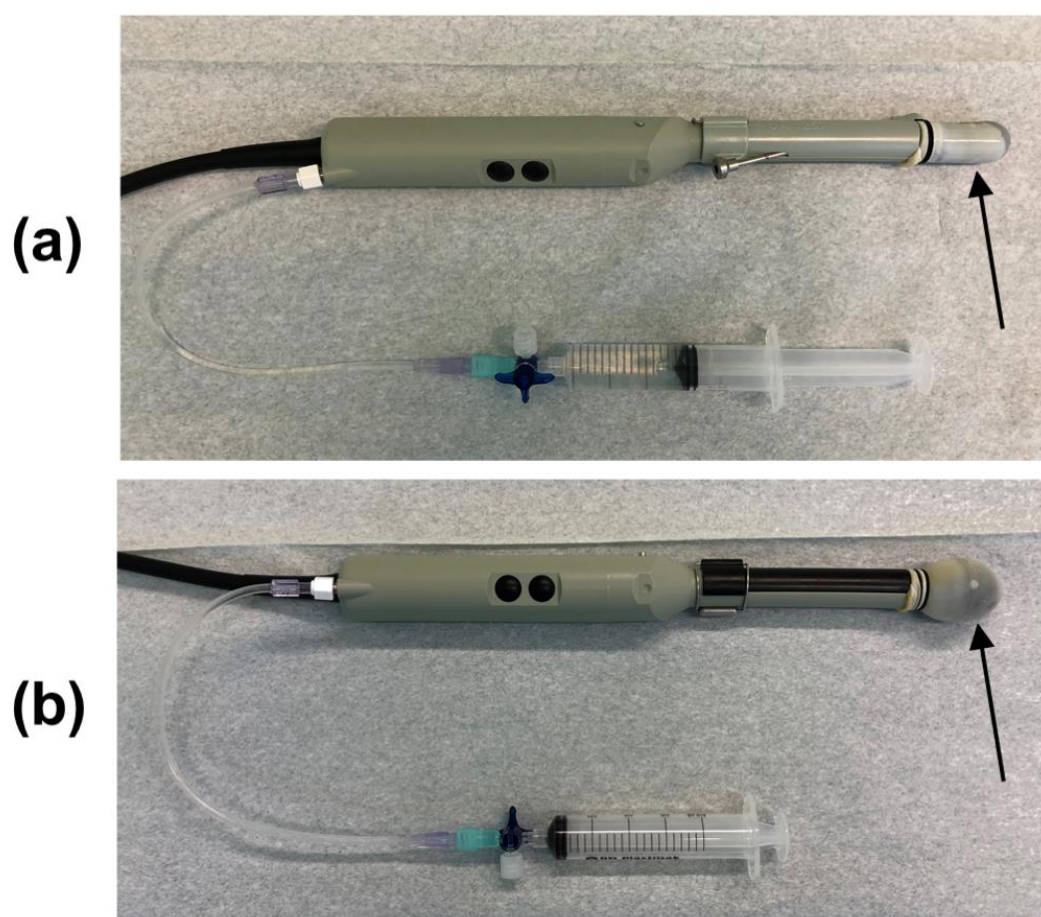


Fig. 7 Ultrasound transducer with empty and filled water standoff. **(a)** Probe mounted with empty water standoff and a biopsy channel bracket (side-fire configuration). **(b)** Probe mounted with filled water standoff and a dummy channel bracket.

(2) Preparation

Before the examination, patients were inquired about their age, recent PSA value (usually tested within recent three months), family history of PCa, history of prostate biopsy, and history of prostate surgery or other treatments, etc. If necessary, blood sample would be taken by the nurse prior to the DRE for a new PSA testing. A questionnaire was issued to obtain the International Prostate Symptom Score (IPSS).

Patients were informed to empty the bowels naturally. Administration of laxatives the day before is unnecessary, because this could even lead to less favorable examination conditions as liquid stool may leak from the sigmoid colon and get caught between the transducer and the rectum, thus leading to unsatisfying imaging quality of the prostate [27]. Besides, a full bladder may contribute to optimizing the imaging quality and better distinguishing the anatomic structures such as the bladder neck on sagittal plane.

(3) Positioning

Generally, patients were placed in the left lateral decubitus position with knees and hips flexed 90 degrees, for the right-handed examiners. In this position, any air bubbles that may be caught in the water-filled standoff would not block the US view of the prostate [27]. Patient's buttocks should be flush with the end of the examination table, enabling the DRE and manipulation of the US probe or biopsy gun without obstruction.

(4) Palpation (DRE)

Patients were informed to relax and take a deep breath when the DRE began. The operator gently inserted his gloved, lubricated index finger (with nails trimmed appropriately) into patient's rectum to determine the size of the prostate and feel for pain, texture (e.g. soft or hard), lumps or other abnormalities. Additionally, abnormal mass in the anus or rectum or blood on the glove would be equally paid close attention to.

(5) Ultrasonography

All the examinations as well as the previous DRE and, if necessary, the subsequent prostate biopsy, were performed by two senior urologists in a dedicated TRUS room. During the procedure, patients could watch the synchronized video of TRUS imaging on a separate monitor under the operator's explanation. The operator gently inserted the condom-covered, lubricated US probe into patient's rectum. Firstly, the whole prostate (especially the PZ, where 70–80% of all carcinomas originate [28]) was inspected for hypoechoic lesions and contour abnormalities (Fig. 8a). The relevant anatomy (e.g. bladder, urethra, ejaculatory ducts, seminal vesicles, rectal wall, etc.) were fully visualized too (Fig. 8b, c). Color Doppler imaging was utilized to depict the velocity and direction of blood flow within the gland and explain asymmetry by vessels (especially in the region of the neurovascular bundle) not to confuse with malignant causes (Fig. 8d).

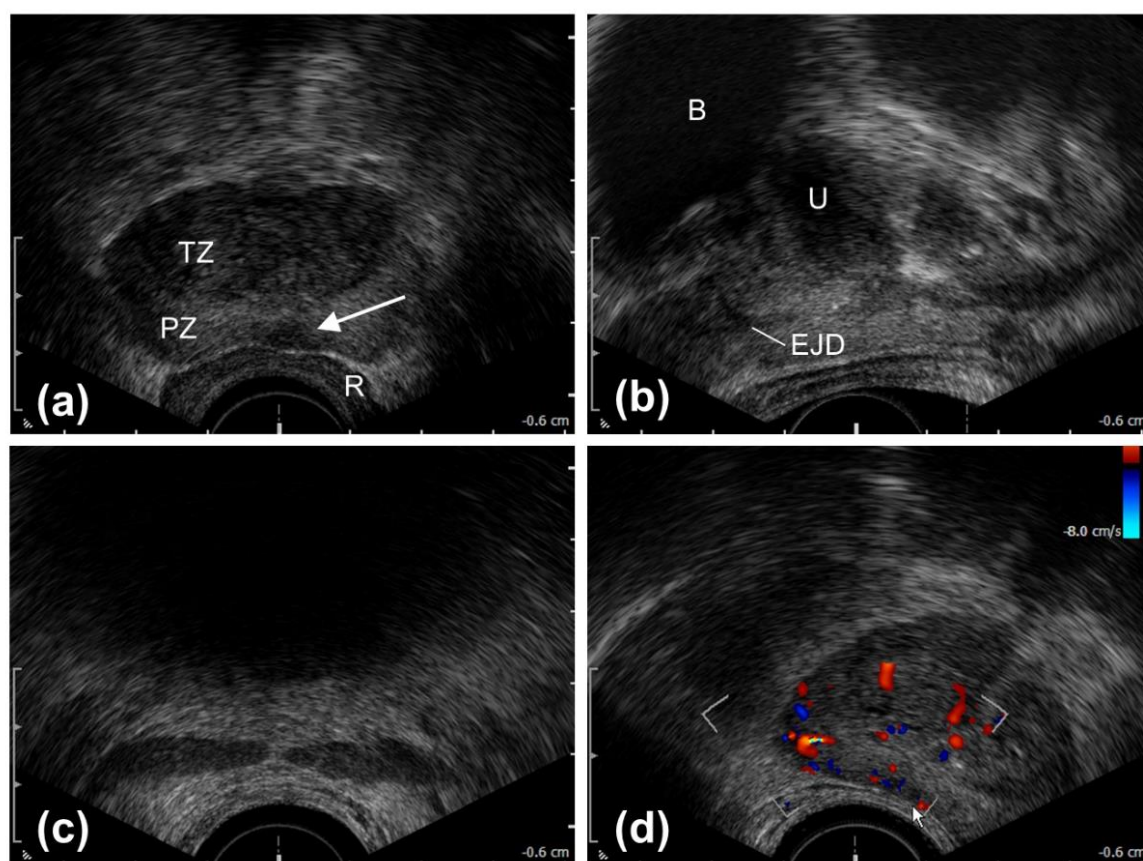


Fig. 8 A “survey” scan of the prostate. (a) Transverse view. TZ, transitional zone; PZ, peripheral zone; R, rectal wall; hypoechoic lesion (*white arrow*). (b) Sagittal view. B, bladder; U, urethra; EJD, ejaculatory ducts. (c) Seminal vesicles. (d) Color Doppler imaging.

After measurement of the three largest diameters (the width and the height in transverse plane, and the length in sagittal plane), the prostate volume was automatically calculated by integrated computing software in the US device (Fig. 9), according to the ellipsoid formula: $\text{volume (mL)} = \text{width (cm)} \times \text{height (cm)} \times \text{length (cm)} \times \pi/6$ [29].

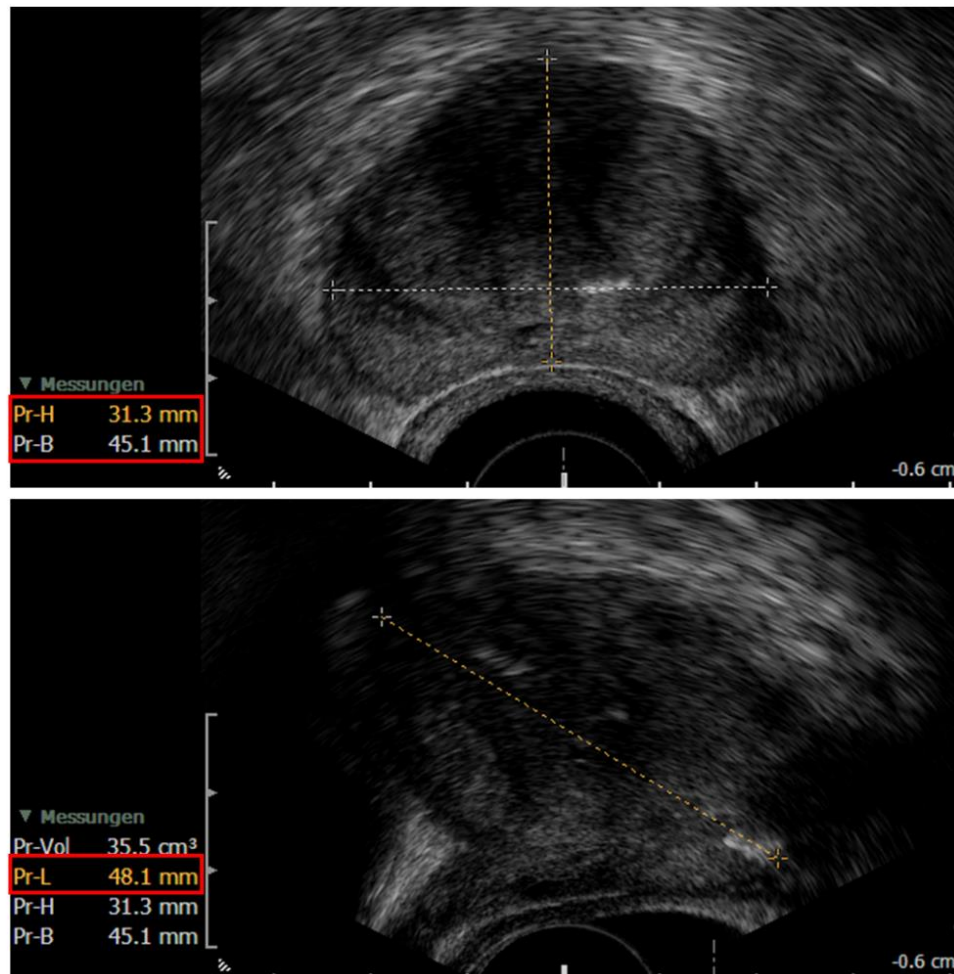


Fig. 9 Volume measurement of the prostate. The width and the height measured in transverse plane (*top*) and the length measured in sagittal plane (*below*).

Transverse TRUS images were manually collected, consecutively starting from the prostate apex and proceeding cephalad until the seminal vesicles were reached, at approximately 5 mm intervals, which is the radius of a tumor volume (0.5 mL) commonly considered as the threshold for clinically significant PCa [30, 31]. The biplane US transducer also allows

sagittal measurements of landmarks and slice thicknesses control. Usually three to ten images were generated depending on the prostate size. Suitable cross-sections contain TRUS-identifiable Internal Landmarks, which are structures with remarkable features in the prostate, including calcifications, cysts, asymmetries, lesions, anatomies (e.g. seminal colliculus, urethra, vessel, etc.) or even resection holes of TURP, ensuring that locating of these selected landmarks could be successfully repeated. Internal Landmarks determined as the anchor points in the first AI-US-CT session are the bases for Trend Monitoring in the subsequent sessions. In the process of Trend Monitoring, new serial TRUS images were obtained in one-to-one correlation with each cross-section scanned in the previous examinations, according to Internal Landmarks (Fig. 10). The date of the correlated previous examinations, the number of the total and the correlated TRUS images in Trend Monitoring sessions, and the type of Internal Landmarks utilized for imaging correlation and their respective number were recorded for the final calculation.

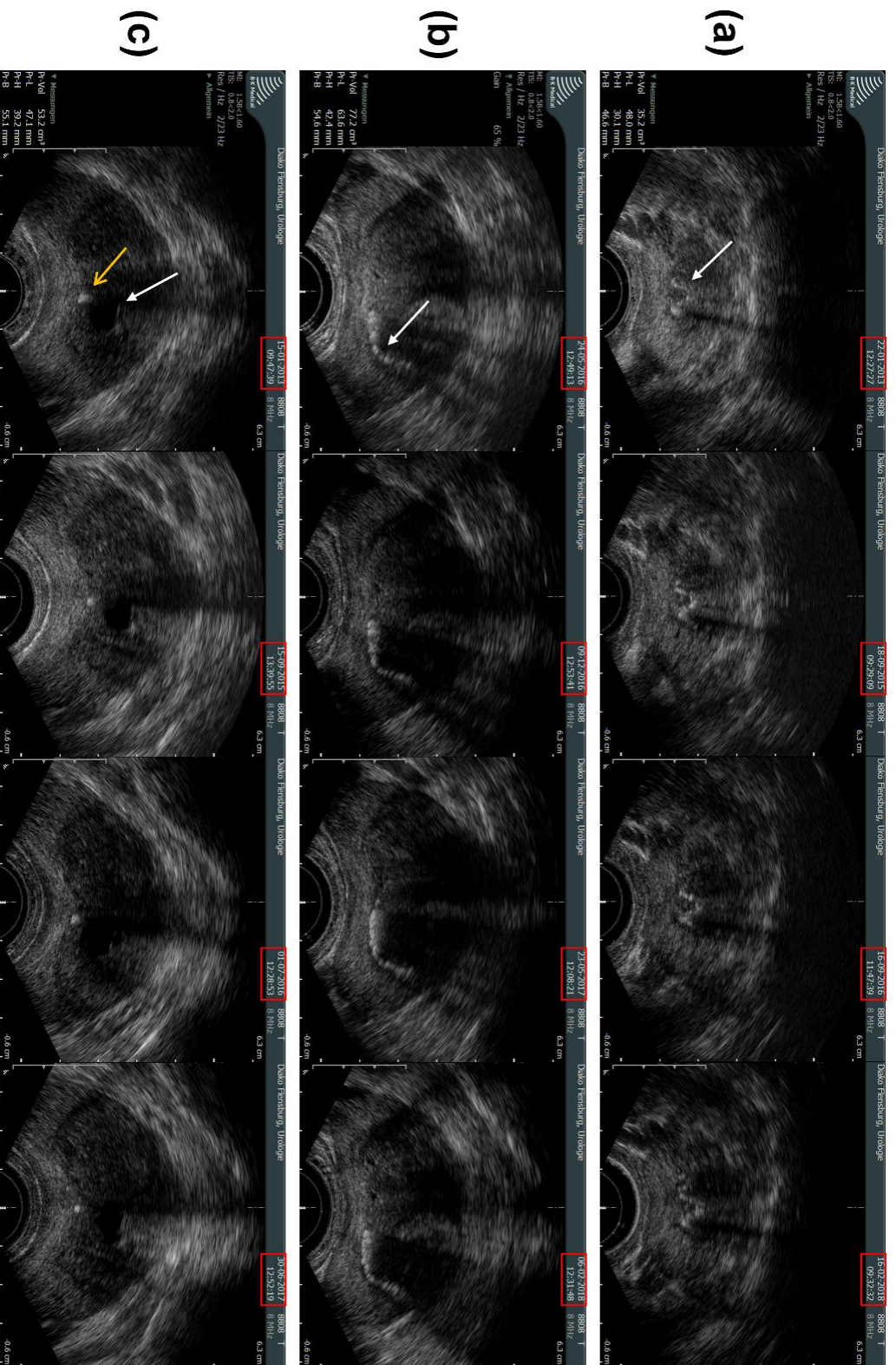


Fig. 10 Image correlation basing on various Internal Landmarks over time. (a) By seminal colliculus (white arrow) on 01/2013, 09/2015, 09/2016, 02/2018. (b) By calcification (white arrow) on 05/2016, 12/2016, 01/2017, 02/2018. (c) By cyst (white arrow) and calcification (yellow arrow) on 01/2013, 09/2015, 07/2016, 06/2017.

(6) ANNA online big data cloud solution

The static TRUS images were digitally stored in BMP format (having no imaging quality loss to the original freeze frame), exported without patient's ID by a dedicated USB flash drive from the US instrument to a password-protected computer, and uploaded to the ANNA server (ANNA/C-TRUS GmbH, Germany) for documentation and analyzation. The operator visited the official website (<http://www.anna-ctrus.de/>) and logged in his own user account through the portal "Login ANNAcTRUS V2". The patient's individual record was accessed (or created, if in the first session) and an item of the new examination was added in. The serial transverse TRUS images were listed in sequence by the time they were generated, labeled to indicate their longitudinal distance to the prostate apex. The prostate apex was designated as level 00, so these images were labeled cephalad to the prostate base as 05, 10, 15, 20, 25, etc. TRUS image of the seminal vesicles indicated the end of a complete collection but did not need to be uploaded for evaluation. All data were transmitted via an encrypted connection, and the ANNA server stored and processed them under pseudonyms. The AI algorithms based on big data (previously described in the introduction part) automatically evaluated the digital US signal information, and tumor suspicious areas were marked by superimposed red color on the original gray-scale TRUS images (Fig. 11). Duration of the analyzing procedure depends on the number of the assessed images, but usually accomplished within three minutes. Patients with elevated or normal PSA value were suggested to revisit after 6 or 12 months, respectively.

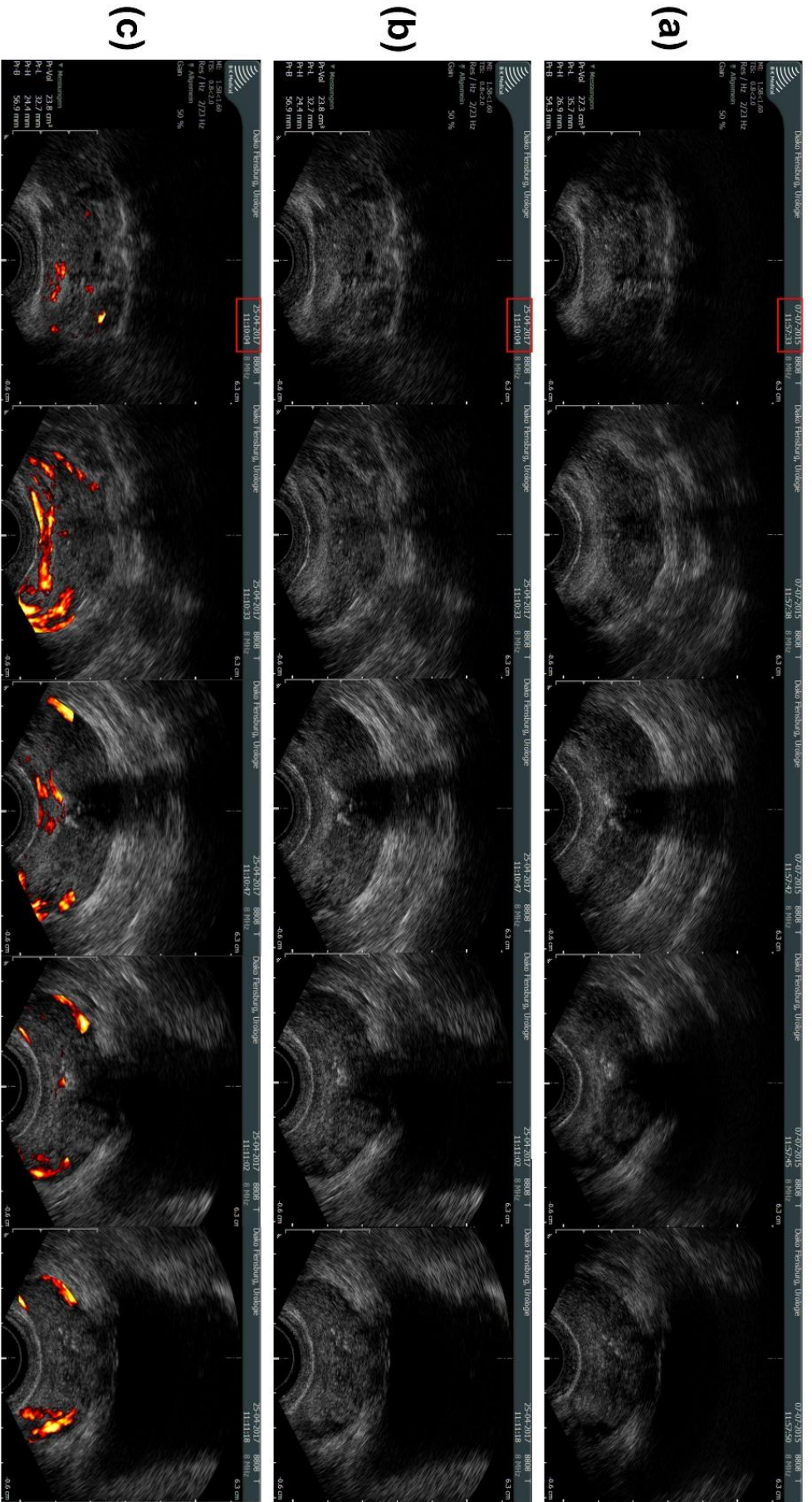


Fig. 11 Depiction of AI-US-CT. Two exactly correlated series of TRUS images on (a) 06/2015 and (b) 04/2017. (c) Session of 04/2017 with ANNA/C-TRUS evaluation.

(7) Biopsy

If indicated, prostate biopsy could be performed immediately after the image analysis. The need for initial biopsy is based on PSA level (> 4 ng/mL) and/or suspicious DRE and/or imaging; the indications for repeat biopsy are rising and/or persistently elevated PSA, suspicious DRE and/or imaging, atypical small acinar proliferation (ASAP) or extensive (multiple biopsy sites) high-grade prostatic intraepithelial neoplasia (HGPIN) in previous biopsies [6]. Patient's wish (e.g. undergoing biopsy or keeping further observation) would also be taken into consideration. Contraindications include significant coagulopathy, acute prostatitis, and severe immunosuppression, etc.

Prophylactic oral antibiotics (Ciprofloxacin, CiproHEXAL[®], Hexal AG, Germany) were given according to the existing guidelines at the time. Sterile biopsy needle, biopsy channel bracket, needle guide, transducer cover, and lubricating gel were utilized. All biopsies were performed via transrectal approach by a side-fire probe (Fig. 7a) with a spring-driven 18-gauge needle core biopsy gun (CORAZOR[®], UROMED Kurt Drows KG, Germany) (Fig. 12).



Fig. 12 Biopsy gun and biopsy samples. Papers were used to record the sampling order and site, keeping the biopsy tissues stretched and flat. Then they were placed in formalin in corresponding jars numbered with biopsy sites.

Patients were informed about the guideline conformed biopsy method. Those who specifically want the targeted biopsies gave their informed consent of taking six-core ANNA/C-TRUS guided biopsy instead of the conventional 10–12 core systematic random biopsy. The ANNA targeted biopsies follow the guideline in procedure aspects. Generally, a maximum of six most tumor-suspicious areas were planned as targets, basing on the ANNA results (i.e. the color-coded TRUS images) in addition to visual hypoechoic lesions. In case of obvious cancer suspicious DRE or TRUS, direct targeted biopsies were performed. For patients in Trend Monitoring, comparison of the image changes in the grey-scale and analysis changes between current and former images could also be considered to help determine the biopsy sites (Fig. 13).

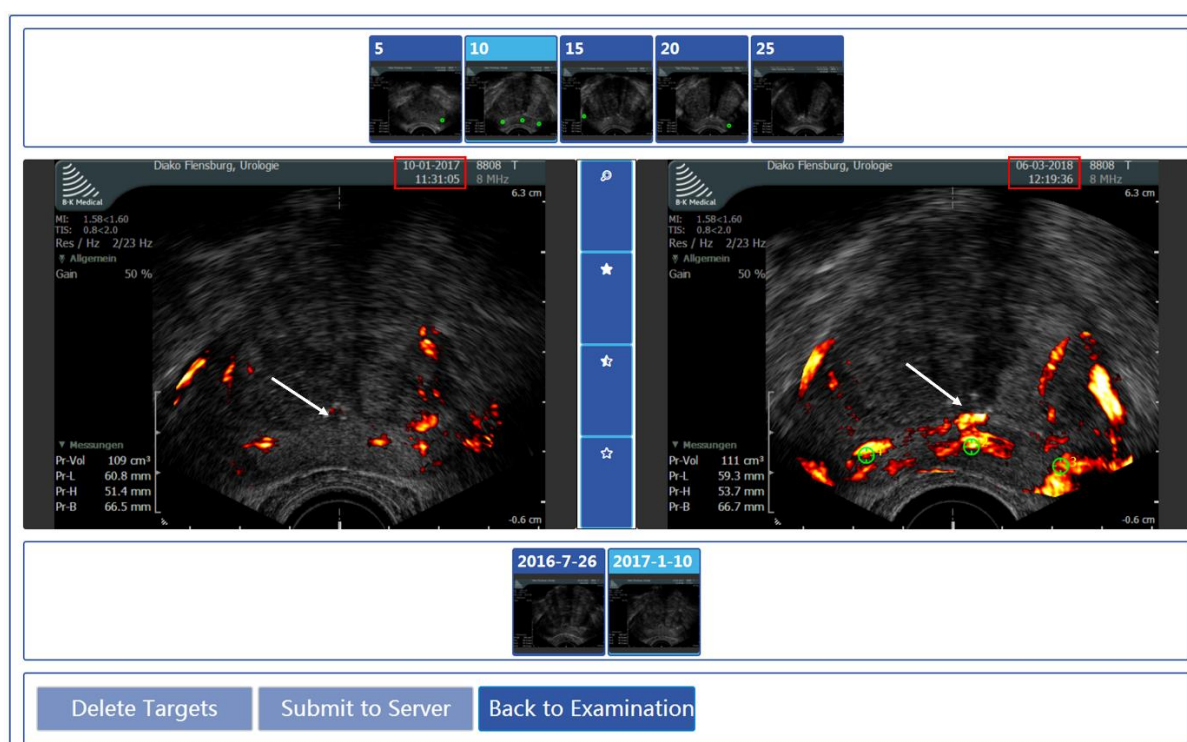


Fig. 13 ANNA results changes in longitudinal follow-up. Transverse TRUS images obtained on 01/2017 (*left*) and 03/2018 (*right*). Internal Landmarks (*white arrow*), i.e. calcifications in this case, indicate the same cross-section (10 mm from the prostate apex). Biopsy shots (*green circle*) were taken on the progression sites and all three turned out to be carcinoma-positive (second shot Gleason Score [GS] = 3 + 3, third shot GS = 3 + 3, fourth shot GS = 4 + 3).

During the biopsy procedure, the biplane probe provided simultaneous visualization of the prostate in both the transverse and sagittal planes (Fig. 14). The pre-planned targets were confirmed by relating them to Internal Landmarks (Internal Fusion) in the transverse plane under real-time visual control [21] and normally one core per lesion was taken to obtain satisfactory tissue (Fig. 14). Patients were informed about the attentions and monitored for possible complications e.g. bleeding, infection, acute urinary retention, etc.

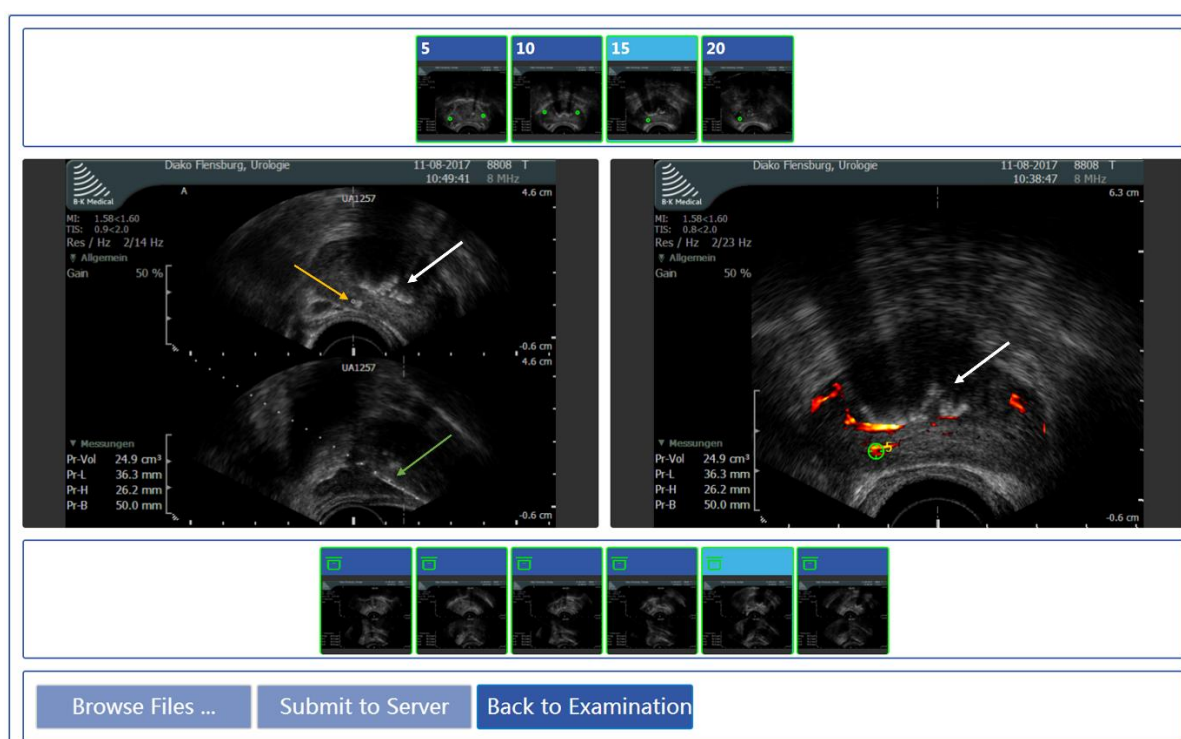


Fig. 14 “Internal Fusion”. Internal Landmarks (*white arrow*), i.e. calcifications in this case, help to locate the planned targets during the process of operation: the pre-planned target based upon ANNA results (*green circle*); the actual biopsy site marked in transverse plane (*yellow arrow*); the actual biopsy needle path in sagittal plane (*green arrow*). Histopathology proved to be carcinoma-positive (GS = 3 + 3).

The biopsy samples were placed in 4% formalin in separated jars (Fig. 12) and sent for histopathological examination. Each biopsy site was reported individually by senior pathologists in our hospital (normally within ten days), including its location, core length, and, if carcinoma-positive, primary and secondary Gleason grade, International Society of Urological Pathology (ISUP) 2014 grade, and carcinoma percentage, etc. Shot images (actual

biopsy needle path in the transverse and sagittal planes) and histopathological findings were documented respectively, and each could be reviewed correlating to their own biopsy sites exactly (Fig. 14, 15).

<input type="checkbox"/> Benigne	Core length	9	(mm)
2	Pattern I	Pattern II	Score
	3	3	6
	Cancer amount	1	(mm)
	Offset from tip	0	(mm)
<input type="checkbox"/> Benigne	Core length	14	(mm)
3	Pattern I	Pattern II	Score
	3	3	6
	Cancer amount	4	(mm)
	Offset from tip	0	(mm)
<input type="checkbox"/> Benigne	Core length	10	(mm)
4	Pattern I	Pattern II	Score
	4	3	7b
	Cancer amount	6	(mm)
	Offset from tip	0	(mm)

Prev 2/5 Next Submit to Server Back to Examination

Fig. 15 Documentation of biopsy data. The biopsy core position (fourth shot of this case) (*red circle*) and its corresponding shot image (*black arrow*) and histopathological findings (*red arrow*).

2.2.2.3. Data collection and statistical calculation

The aim of the statistical calculation is to evaluate the feasibility of Internal Landmarks in assistance for Trend Monitoring and targeted biopsy by ANNA/C-TRUS.

Collected data included patients' number, age, prostate volume, serum PSA value (free and total), IPSS, individual AI-US-CT sessions and time intervals, family history of PCa, history of prior biopsies and prostate treatments, abnormal findings of DRE, number of Internal Landmarks, number of TRUS images (correlated and total), number of patients accepted

targeted biopsy (initial and repeat), number of PCa detected, GS and ISUP grade, number of individual biopsy cores (positive and total), etc.

Relevant formulas are as follows:

- (1) PSAD (ng/mL/cm^3) = PSA/prostate volume;
- (2) PSAV (ng/mL/year) = $[(\text{PSA2} - \text{PSA1}) + (\text{PSA3} - \text{PSA2})]/2$ (PSA1, PSA2, PSA3: at least 3 serum PSA values tested within 2 years);
- (3) f/t PSA ratio = free PSA/total PSA;
- (4) Imaging correlation rate = correlated TRUS images/total TRUS images;
- (5) PCa detection rate = PCa detected/total patients;
- (6) Biopsy positive rate = positives cores/total cores;
- (7) Average cores detecting one PCa = total cores/PCa detected.

All the statistical evaluation and graphical representation of the collected data was performed with Microsoft Excel 2016 and Word 2016 (Microsoft, USA).

3. Results

3.1. Landmarks validation in vitro

In the simulation setting in vitro, cross-sections of a prostate phantom could be re-identified and re-located in 121 out of 121 TRUS images, correlating to fixed-size artificial anchor points (Internal Landmarks), even by utilizing four various models of US instruments and probes with respective parameter settings, by two urologists at different times (Table 1).

Table 1 Landmarks validation in vitro

$N = 121$	Transversal correlation		Longitudinal correlation	
	Metal cylinder	Air bubble	Metal cylinder	Air bubble
BK 1				
Doctor 1	8	8	4	4
Doctor 2	2	2	1	1
BK 2				
Doctor 1	6	6	3	3
Doctor 2	4	4	2	2
BK 3				
Doctor 1	8	8	4	4
Doctor 2	4	4	2	2
BK 4				
Doctor 1	4	4	2	2
Doctor 2	5	4	2	2

Number of TRUS images correlated by fixed-size artificial Internal Landmarks (metal cylinder and air bubble) in an US prostate phantom, respectively by two urologists at different times, on four US equipment.

BK 1: Pro Focus 2202, transducer 8808 at 8 MHz; *BK 2*: Viking 2400, transducer 8808 at 8 MHz; *BK 3*: Pro Focus 2202, transducer 8818 at 12 MHz; *BK 4*: bk5000, transducer E14C4t at 9 MHz

3.2. Landmarks study in vivo

3.2.1. Landmarks in single AI-US-CT session

By exact correlations of Internal Landmarks, even under the size of one-millimeter, an accurate re-identification and re-location of the identical cross-sections of the prostate for obtaining precisely matched TRUS images within one single AI-US-CT session was possible. Even after repositioning the US transducer (i.e. rotating, angling, or cephalad and caudally moving) by different junior or senior urologists at different times, accurate correlation was still possibly achieved (Fig. 6, 16).

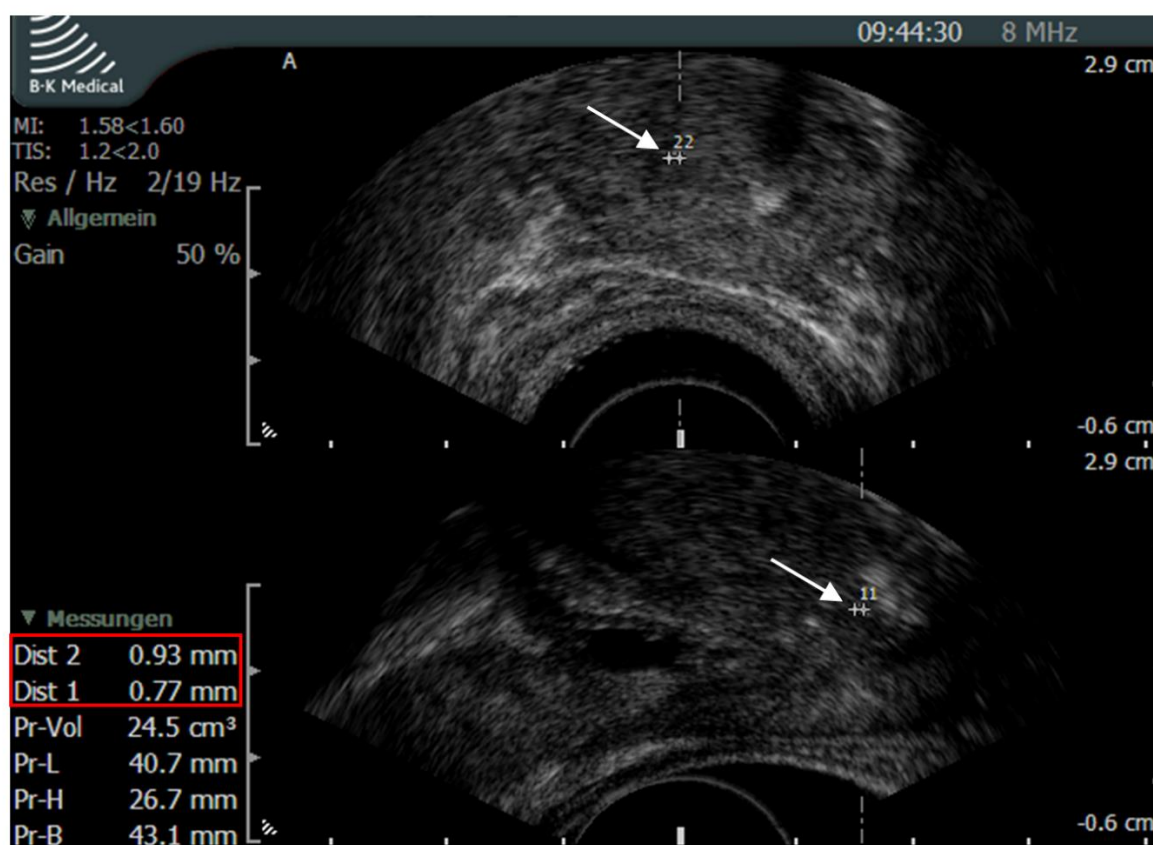


Fig. 16 Internal Landmarks in vivo. Calcification under one-millimeter (red box) located and measured in both transverse (*top*) and sagittal (*below*) TRUS planes.

3.2.2. Landmarks in multiple AI-US-CT sessions (Trend Monitoring)

3.2.2.1. General clinical characteristics

From January 2017 to May 2018, a total of 164 patients were included for this observational study, and none of them met the exclusion criteria.

Of all the 164 patients under Trend Monitoring, eight men (5%) had been diagnosed with PCa before the inclusion and underwent radiotherapy, hormonal therapy, or focal therapy e.g. high-intensity focused ultrasound (HIFU); eighty-seven men (53%) were suspicious of PCa and a third of them (29 men) chose ANNA/C-TRUS guided biopsy; the rest 69 men (42%) came for mere prevention or early detection (Fig. 17).

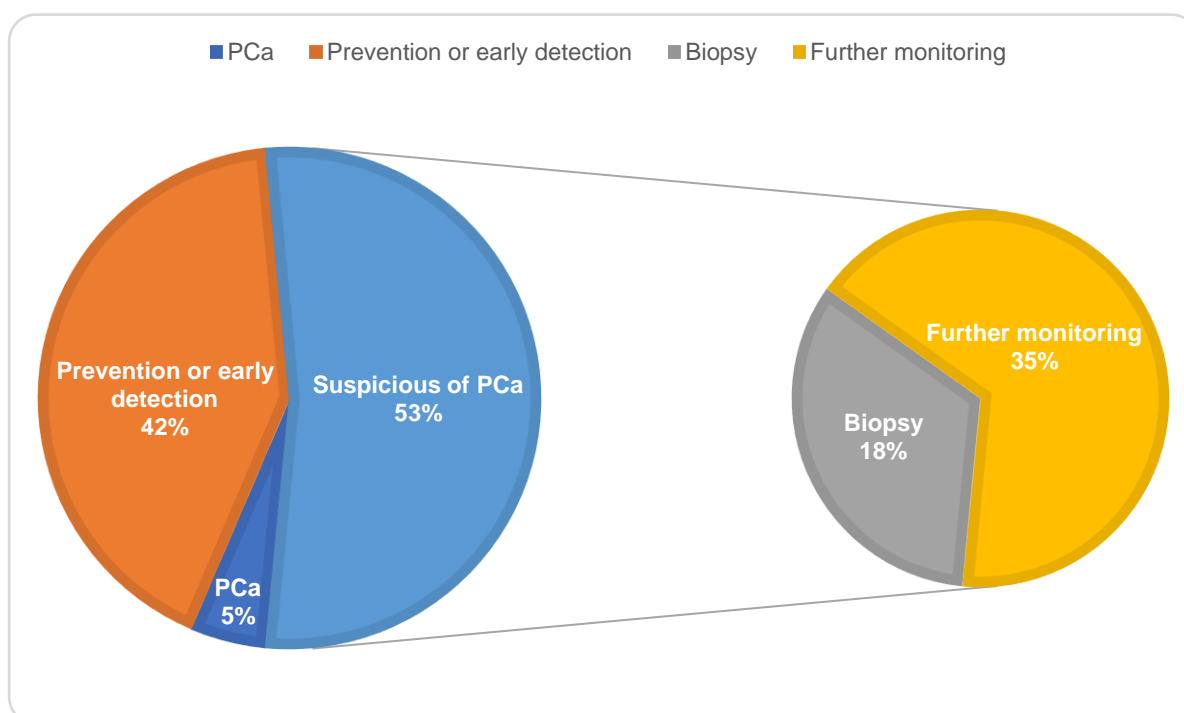


Fig. 17 Distribution Characteristics of patients under Trend Monitoring.

The consecutive 164 patients had an age ranged from 46–89 years with a median of 73 years. The TRUS prostate volume ranged from 7.72–272 mL with a median of 41 mL. The serum PSA value ranged from 0.02–48.96 ng/mL with a median of 3.75 ng/mL. The PSA density

(PSAD) ranged from 0.001–0.53 ng/mL/cm³ with a median of 0.09 ng/mL/cm³. The free/total PSA ratio (f/t PSA) ranged from 0.06–0.6 with a median of 0.27. The PSA velocity (PSAV) ranged from -13.83–8.54 ng/mL/year with a median of 0.09 ng/mL/year. The IPSS ranged from 0–27 with a median of 8. The number of individual total AI-US-CT sessions ranged from 2–21 with a median of 5. The number of individual AI-US-CT sessions during the current study ranged from 1–4 with a median of 2. The time interval between first and latest session ranged from 1–113 months with a median of 50 months. Thirty-two patients (20%) had a family history of PCa. Ninety-two patients (56%) had prior negative biopsies, e.g. systematic random biopsy, mpMRI guided biopsy or even transperineal saturation biopsy under general anesthesia with up to 80 cores. Twenty-three patients (14%) had a history of prostatic surgeries including TURP and prostate adenoma enucleation (PAE). Six patients (4%) had an abnormal DRE (Table 2).

Of the 8 patients who had been diagnosed with PCa before the inclusion, their age ranged from 67–87 years with a median of 80 years. The TRUS prostate volume ranged from 9.96–59.3 mL with a median of 17.4 mL. The serum PSA value ranged from 0.02–6.73 ng/mL with a median of 1.72 ng/mL. The PSAD ranged from 0.001–0.33 ng/mL/cm³ with a median of 0.1 ng/mL/cm³. The f/t PSA ranged from 0.06–0.33 with a median of 0.15. The PSAV ranged from -1.22–3.25 ng/mL/year with a median of 0.07 ng/mL/year. The IPSS ranged from 2–27 with a median of 7. The number of individual total AI-US-CT sessions ranged from 3–18 with a median of 4. The number of individual AI-US-CT sessions during the current study ranged from 1–3 with a median of 2. The time interval between first and latest session ranged from 11–105 months with a median of 35.5 months. Three patients (38%) had a family history of PCa. One patient (13%) had a history of TURP or PAE. Two patients (25%) had an abnormal DRE (Table 2).

Of the 87 patients suspicious of PCa, their age ranged from 56–89 years with a median of 74 years. The TRUS prostate volume ranged from 7.72–272 mL with a median of 50.4 mL. The serum PSA value ranged from 0.25–48.96 ng/mL with a median of 6.15 ng/mL. The PSAD ranged from 0.02–0.53 ng/mL/cm³ with a median of 0.12 ng/mL/cm³. The f/t PSA ranged

from 0.09–0.56 with a median of 0.23. The PSAV ranged from -13.83–8.54 ng/mL/year with a median of 0.15 ng/mL/year. The IPSS ranged from 0–24 with a median of 9. The number of individual total AI-US-CT sessions ranged from 2–21 with a median of 7. The number of individual AI-US-CT sessions during the current study ranged from 1–4 with a median of 2. The time interval between first and latest session ranged from 1–113 months with a median of 69 months. Fifteen patients (17%) had a family history of PCa. Sixty-eight patients (78%) had prior negative biopsies. Thirteen patients (15%) had a history of TURP or PAE. Four patients (5%) had an abnormal DRE (Table 2).

Of the 69 patients who came for mere prevention or early detection, their age ranged from 46–82 years with a median of 71 years. The TRUS prostate volume ranged from 10.4–103 mL with a median of 35.7 mL. The serum PSA value ranged from 0.1–4.33 ng/mL with a median of 1.71 ng/mL. The PSAD ranged from 0.01–0.22 ng/mL/cm³ with a median of 0.05 ng/mL/cm³. The f/t PSA ranged from 0.07–0.6 with a median of 0.30. The PSAV ranged from -3.12–0.64 ng/mL/year with a median of 0.003 ng/mL/year. The IPSS ranged from 0–24 with a median of 8. The number of individual total AI-US-CT sessions ranged from 2–14 with a median of 4. The number of individual AI-US-CT sessions during the current study ranged from 1–3 with a median of 1. The time interval between first and latest session ranged from 1–110 months with a median of 42 months. Fourteen patients (20%) had a family history of PCa. Twenty-four patients (35%) had prior negative biopsies. Nine patients (13%) had a history of TURP or PAE (Table 2).

Table 2 Patient demographics

	All patients	PCa	Abnormal PSA/DRE/TRUS	Prevention
Patients number	164	8	87	69
Age (years)				
Median	73	80	74	71
Range	46–89	67–87	56–89	46–82
Volume (mL)				
Median	41	17.4	50.4	35.7
Range	7.72–272	9.96–59.3	7.72–272	10.4–103
PSA (ng/mL)				
Median	3.75	1.72	6.15	1.71
Range	0.02–48.96	0.02–6.73	0.25–48.96	0.1–4.33
PSAD (ng/mL/cm ³)				
Median	0.09	0.1	0.12	0.05
Range	0.001–0.53	0.001–0.33	0.02–0.53	0.01–0.22
f/t PSA				
Median	0.27	0.15	0.23	0.30
Range	0.06–0.6	0.06–0.33	0.09–0.56	0.07–0.6
PSAV (ng/mL/year)				
Median	0.09	0.07	0.15	0.003
Range	-13.83–8.54	-1.22–3.25	-13.83–8.54	-3.12–0.64
IPSS				
Median	8	7	9	8
Range	0–27	2–27	0–24	0–24
Sessions (total)				
Median	5	4	7	4
Range	2–21	3–18	2–21	2–14
Sessions (current study)				

Median	2	2	2	1
Range	1–4	1–3	1–4	1–3
Session interval (months)				
Median	50	35.5	63	42
Range	1–113	11–105	1–113	1–110
Family history of PCa	32 (20%)	3 (38%)	15 (17%)	14 (20%)
Prior negative biopsies	92 (56%)	–	68 (78%)	24 (35%)
History of prostate surgeries	23 (14%)	1 (13%)	13 (15%)	9 (13%)
Abnormal DRE	6 (4%)	2 (25%)	4 (5%)	–

Clinical characteristics of all 164 patients, and respectively of 8 patients with PCa, 87 patients suspicious of PCa, and 69 patients came for mere prevention or early detection

3.2.2.2. Characteristics of landmarks

Overall, a total of 1846 Internal Landmarks were utilized as anchor points during the process of Trend Monitoring, including prostatic calcifications (1128, 62%), cysts (524, 28%), seminal colliculus (133, 7%) and others (61, 3%). Basing on re-locating of the Internal Landmarks, accurate imaging correlations were attained in 1021 out of 1090 TRUS slices (94%), after years, despite volume changes, even generated on different US instruments by different operators (Fig. 18) (Table 3). The longest Trend Monitoring with accurate image correlation in current study had so far reached 9 years and 5 months (Fig. 19).

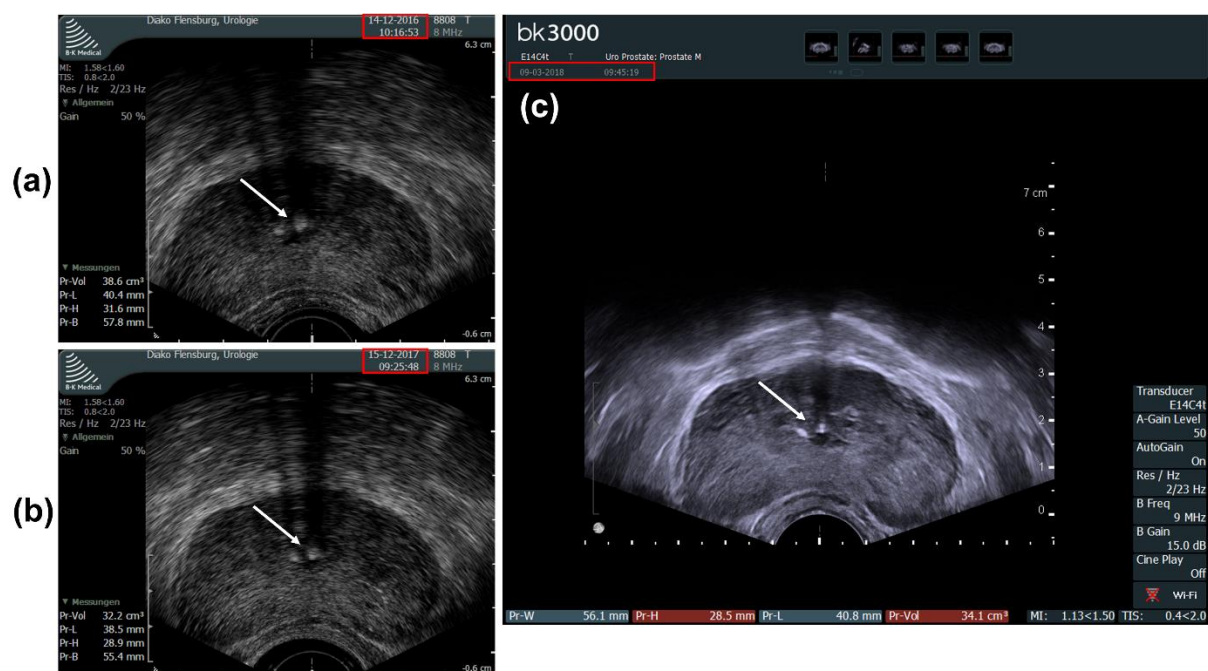


Fig. 18 Re-identifying of the cross-sections by Internal Landmarks in Trend Monitoring. Internal Landmarks (*white arrow*) help to locate the same cross-section of the prostate (20 mm from the prostate apex) over time. (a) Transverse TRUS image attained in 2016, on Pro Focus 2202 with transducer 8808 at 8 MHz, by doctor 1. (b) Transverse TRUS image of the same cross-section in (a) attained in 2017, on Pro Focus 2202 with transducer 8808 at 8 MHz, by doctor 2. (c) Transverse TRUS image of the same cross-section in (a) attained in 2018, on bk3000 with transducer E14C4t at 9 MHz., by doctor 1.

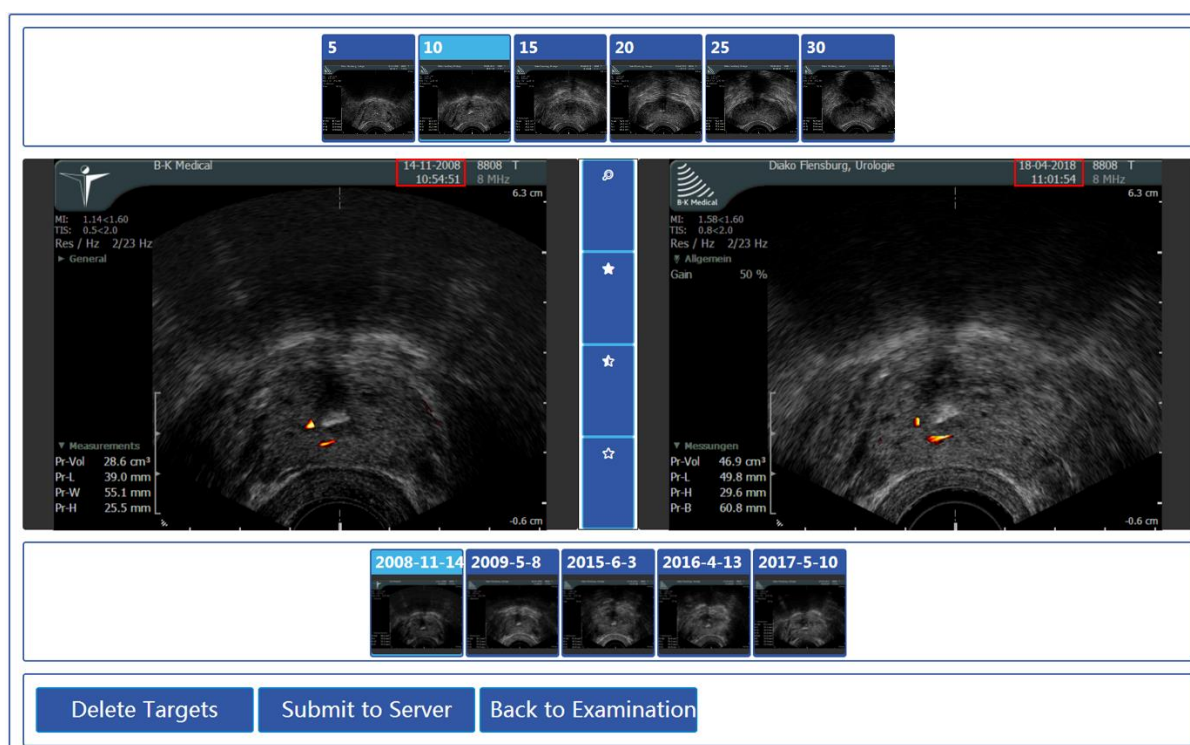


Fig. 19 Long-term Trend Monitoring with accurate image correlation. TRUS images of the identical cross-section (10 mm from the prostate apex) obtained from 11/2008 (*left*) to 04/2018 (*right*). With an interval of 9 years and 5 months, although the prostate volume increased from 29 mL to 47 mL, accurate imaging correlation was still made based on Internal Landmarks. The PSA value ranged from 5.31 ng/mL (2008) to 5.45 ng/mL (2018), meanwhile no significant progression in AI-US-CT analysis pattern was found, and prior biopsies proved to be carcinoma-negative.

Of the 8 patients who had been diagnosed with PCa before the inclusion, a total of 74 Internal Landmarks were utilized, including prostatic calcifications (33, 45%), cysts (8, 11%), seminal colliculus (2, 3%) and others (31, 41%), to facilitate accurate imaging correlations in 46 out of 53 TRUS slices (87%) during the process of Trend Monitoring (Table 3).

Of the 87 patients suspicious of PCa, a total of 1128 Internal Landmarks were utilized, including prostatic calcifications (704, 62%), cysts (313, 28%), seminal colliculus (91, 8%) and others (20, 2%), to facilitate accurate imaging correlations in 637 out of 681 TRUS slices (94%) (Table 3).

Of the 69 patients who came for mere prevention or early detection, a total of 644 Internal Landmarks were utilized, including prostatic calcifications (391, 61%), cysts (203, 32%), seminal colliculus (40, 6%) and others (10, 1%), to facilitate accurate imaging correlations in 338 out of 356 TRUS slices (95%) (Table 3).

Table 3 Characteristics of correlated Internal Landmarks and TRUS images in follow-up

	All patients	PCa	Abnormal PSA/DRE/TRUS	Prevention
Correlated Internal Landmarks				
Total	1846	74	1128	644
Calcifications				
Number	1128	33	704	391
Rate	62%	45%	62%	61%
Cysts				
Number	524	8	313	203
Rate	28%	11%	28%	32%
Seminal colliculus				
Number	133	2	91	40
Rate	7%	3%	8%	6%
Others				
Number	61	31	20	10
Rate	3%	41%	2%	1%
Correlated transverse TRUS images				
Correlated/total	1021/1090	46/53	637/681	338/356
Correlation rate	94%	87%	94%	95%

Characteristics of correlated Internal Landmarks and TRUS images during the process of Trend Monitoring of all 164 patients, and respectively of 8 patients with PCa, 87 patients suspicious of PCa, and 69 patients came for mere prevention or early detection

3.2.2.3. Characteristics of targeted biopsies

Of the 87 patients suspicious of PCa, twenty-nine men (33%) chose ANNA/C-TRUS targeted biopsy. A total of 358 Internal Landmarks were utilized, including prostatic calcifications (225, 64%), cysts (87, 24%), seminal colliculus (41, 11%) and others (5, 1%), to facilitate accurate imaging correlations in 211 out of 228 TRUS slices (93%), and non-visual lesions in gray-scale US were detected as PCa in 15 out of 29 patients (52%), including 9 men with ISUP grade 1 (GS: $3 + 3 = 6$), two with ISUP grade 2 (GS: $3 + 4 = 7a$), two with ISUP grade 3 (GS: $4 + 3 = 7b$), one with ISUP grade 4 (GS: $3 + 5 = 8$) and 1 with ISUP grade 5 (GS: $4 + 5 = 9$). Individual punctures ranged from 2–6 cores with a median of 6 cores. Totally 151 cores were performed to achieve 34 positive cores (23%) and PCa were detected on average every 10.1 biopsy cores (Table 4).

In initial biopsy, a total of 91 Internal Landmarks were utilized, including prostatic calcifications (64, 70%), cysts (19, 21%) and seminal colliculus (8, 9%). Totally 56/57 (98%) TRUS images could be correlated due to Internal Landmarks detecting PCa in 7/10 patients (70%), including 6 men with ISUP grade 1 (GS: $3 + 3 = 6$) and 1 with ISUP grade 5 (GS: $4 + 5 = 9$). Individual punctures ranged from 3–6 cores with a median of 6 cores. Totally 57 cores were performed to achieve 15 positive cores (26%) and PCa were detected on average every 8.1 biopsy cores (Table 4).

In repeat biopsy, a total of 267 Internal Landmarks were utilized, including prostatic calcifications (161, 61%), cysts (68, 25%), seminal colliculus (33, 12%) and others (5, 2%). Totally 155/171 (91%) TRUS images could be correlated due to Internal Landmarks detecting PCa in 8/19 patients (42%), including 3 men with ISUP grade 1 (GS: $3 + 3 = 6$), two with ISUP grade 2 (GS: $3 + 4 = 7a$), two with ISUP grade 3 (GS: $4 + 3 = 7b$) and 1 with ISUP grade 4 (GS: $3 + 5 = 8$). Individual punctures ranged from 2–6 cores with a median of 6 cores. Totally 94 cores were performed to achieve 19 positive cores (20%) and PCa were detected on average every 11.8 biopsy cores (Table 4).

Table 4 Characteristics of targeted biopsies

	All biopsy	Initial biopsy	Repeat biopsy
Patients number	29	10	19
Correlated Internal Landmarks			
Total	358	91	267
Calcifications			
Number	225	64	161
Rate	64%	70%	61%
Cysts			
Number	87	19	68
Rate	24%	21%	25%
Seminal colliculus			
Number	41	8	33
Rate	11%	9%	12%
Others			
Number	5	–	5
Rate	1%	–	2%
Correlated transverse TRUS images			
Correlated/total	211/228	56/57	155/171
Correlation rate	93%	98%	91%
PCa detection rate	15/29 (52%)	7/10 (70%)	8/19 (42%)
Gleason Score			
ISUP grade 1	9	6	3
ISUP grade 2	2	–	2
ISUP grade 3	2	–	2
ISUP grade 4	1	–	1
ISUP grade 5	1	1	–
Biopsy cores			
Individual cores			

Median	6	6	6
Range	2–6	3–6	2–6
Positive/total	34/151 (23%)	15/57 (26%)	19/94 (20%)
Cores to detect one PCa	10.1	8.1	11.8

Characteristics of 29 patients who chose ANNA/C-TRUS targeted biopsy during the process of Trend Monitoring, and respectively of 10 patients for initial biopsy and 19 patients for repeat biopsy

4. Discussion

4.1. Study objectives

4.1.1. Current dilemmas and challenges in urologic imaging

Urologic medical imaging, especially ultrasound, is available and being an essential part of the daily clinical practice and playing an important role in the detection of PCa. However, the most widely used imaging technique, gray-scale or regular B-mode US, has limitations on visually distinguishing between benign and malignant prostate tissues. Malignant diseases have various morphology in visual imaging interpretation, while non-malignant conditions such as prostatitis, inflammation, and BPH, can also appear as hypoechoic on US imaging like cancerous tissues [32]. Furthermore, there are no clear standards of how to perform and document a standardized procedure. Thus, innovative imaging and computer analysis modalities are emerging and conventional modalities are being adapted to improve results and broaden the applications.

Compared to regular gray-scale US, MRI for PCa detection has largely followed a multiparametric approach, which incorporates functional sequences (diffusion-weighted imaging and dynamic contrast-enhanced imaging) in addition to high-resolution anatomical sequences (T2-weighted imaging) for imaging the different biological characteristics of the tumor. A number of investigators tried to combine or fuse these multiparametric findings assessing the tissues on MRI with the capability of real-time visualization of TRUS, expecting to help accurately identifying and targeting prostate lesions during biopsy. Commercially marketed MRI/US fusion devices superimpose pre-procedural diagnostic MRI images over real-time US images obtained at a different time and place, assisting pre-planned targets of suspicious areas detected on MRI to be biopsied under real-time US guidance [15, 33]. As a relative concept, we termed this fusion process as “External Fusion”, because an additional

different imaging modality, i.e. mpMRI, is requisite to be provided besides the basic gray-scale TRUS [24].

Instead of taking advantage of the features of external imaging modalities, other investigators tried to further develop the US-based imaging techniques. Prostate HistoScanning (PHS) utilizes statistical analysis of raw backscattered US to pinpoint suspicious prostate lesions [16]. Contrast-enhanced ultrasound (CEUS) imaging detects the increased microvascular density of the tumorous region affected by angiogenesis and disorganized neovascularization [17]. Real-time elastography (RTE) adds computerized information about prostate tissue stiffness under varying degrees of compression to suggest malignancy [18]. ANNA/C-TRUS was established upon a large series of accurately correlated fusion between TRUS images and known pathology of RP specimens. That means this AI algorithm can detect tumor-suspicious areas for targeted biopsies simply by analyzing regular gray-scale TRUS images, and no fusion with an external imaging modality is deemed necessary. Therefore, this technique was termed as “Internal Fusion” [24].

To translate Internal Fusion or External Fusion technique, or any other image-based biopsy methods into clinical application, it needs to be ascertained that the regions marked as cancer-suspicious truly represent the corresponding areas of the prostate and all targets could be hit in their authentic anatomical locations. Furthermore, to obtain meaningful data about the true number of missed PCa, the only feasible option is to follow up for e.g. at least 10 years, which seems prudent to identify the negative effect of a missed tumor. Therefore, it is utmost important to continuously assess a certain cross-section of the prostate and re-locate the same suspicious lesions in a longitudinal observation.

4.1.2. Initial questions of current study

In this study, we hypothesized that natural intraprostatic findings (e.g. calcifications) could possibly function as the similar role in imaging localization as fiducial and radiofrequency markers (e.g. gold seeds) utilized for real-time tumor tracking during radiotherapy for PCa.

To support this hypothesis, two questions were tried to be explained through an observation of the routine clinical practice in our institution:

- (1) How can we re-identify the same cross-section and region of interest (ROI) of the prostate in single TRUS examination and/or in subsequent follow-up sessions? Are TRUS-identifiable intraprostatic morphologic structures, which we termed as “Internal Landmarks”, capable of being utilized as anchor points as we assumed to support accurate localization during the imaging process?
- (2) If so, which specific kind of Internal Landmarks are the most representative to be applied?

4.2. Study findings

4.2.1. Functionality of Internal Landmarks (the first question)

In the simulation setting *in vitro*, we found out that by correlating to immobile fixed-size artificial markers, desired cross-sections of the prostate phantom could all be re-identified under any circumstances (Table 1), even by different operators, utilizing various models of US equipment with respective parameter settings at different times (Fig. 5). The imaging correlation rate *in vitro* (100%) proves that in ideal condition Internal Landmarks are reproducible anchor points to reliably facilitate accurate localization during the imaging process and shows the feasibility and necessity of further observation *in vivo*.

In single TRUS examination (i.e. one AI-US-CT session in this study), we found out that by exact correlations to Internal Landmarks even under the size of one-millimeter (Fig. 16), higher accuracy was achieved to re-identify and re-locate the identical cross-sections of the prostate for obtaining precisely matched TRUS images, even after repositioning the US transducer (i.e. rotating, angling, or cephalad and caudally moving), operated by different junior or senior urologists at different times (Fig. 6). This fact shows that within one single AI-US-CT session, the functionality of Internal Landmarks which has been tested and verified

in phantom could also be successfully reproduced in the real prostate, promoting this study to the next phase of continuous observation in multiple AI-US-CT sessions.

In a series of consecutive TRUS examinations (i.e. multiple AI-US-CT sessions, or Trend Monitoring process in this study), we found out that accurate imaging correlations were attained in 94% of the total 1090 TRUS images collected from 164 patients (Table 3), based on re-locating of the Internal Landmarks, after years, despite prostate volume changes, even generated on different US equipment by different operators (Fig. 18, 19). In this study, the longest time interval between AI-US-CT sessions in the Trend Monitoring process with accurate imaging correlation had so far reached 9 years and 5 months (Fig. 19).

Supported by the zonal anatomy of the prostate as well as the origin of the tumor [34], current guidelines recommend an extended 12-core biopsy that includes a standard sextant sampling of the apex, midgland, and base of both the right and left sides of the prostate, as well as six additional cores from the lateral peripheral zone on each side [9, 35]. The location information of prostate biopsy cores is individually recorded by their anatomic site, i.e. right apex, right mid, right base, right lateral apex, right lateral mid, right lateral base, and, left apex, left mid, left base, left lateral apex, left lateral mid, left lateral base. However, zonal anatomy alone is not enough to help guiding a repeat biopsy precisely to an area which prior negative biopsy had been performed. The description of the biopsy site, e.g. right lateral apex, lacks more detailed information about the actual sampling location, hence it is hardly possible for the operators to continuously identify and assess a same ROI during a long-term monitoring of the prostate.

As an intended improvement to conventional 12-core biopsy, transperineal template guided biopsy utilizes a brachytherapy grid with numerous evenly spaced needle holes so that a systematic and organized approach to prostate tissue sampling is ensured. Location of each individual biopsy core is recorded with its corresponding coordinates which are generally letter-and number-coded on the X- and Y-axis of the brachytherapy grid [36]. To a certain extent, application of the template could possibly reduce the influence from operator and

experience dependent factors of the free-hand biopsy procedure, and the locating method by grid coordinates instead of imaginary prostatic zones is relatively more accurate. However, this method may overlook the effect of prostate volume changes during a long-term monitoring process. In general, prostate volume increases slowly but steadily with advancing age. Rhodes et al. [37] stated that prostate growth followed an exponential growth pattern, with a slope estimate of 0.4 mL/yr for men ages 40 to 59 years at baseline and of 1.2 mL/yr for those 60 to 79 years at baseline. In treatments for lower urinary tract symptoms (LUTS) and BPH, pharmacologic agents suppressing testosterone e.g. finasteride have been shown to reduce prostate size approximately 20–32% [38, 39]. In brachytherapy for PCa, the prostate volume significantly declines, with a 37% and over 50% size reduction at 1 year and 8 years after seeds implantation, respectively [40]. Androgen ablation will cause an average 30% and up to 60% volume decrease in prostates with and without cancer [41]. Apparently, fixed coordinates are unable to truly reflect the relative location changes of the ROI due to prostate size increase or reduction, and any circumstances that would cause prostate deformation. In the natural process or after treatments on prostate, tissues of other areas would be mistakenly assessed instead of the ROI if still being located and guided by the previously recorded template grid coordinates. Observation in current study revealed that in most cases (94%) cross-sections of the prostate under continuous assessments could be repeatedly re-identified by Internal Landmarks even up to a decade (Fig. 10, 18, 19). Therefore, registration of the ROI in correlation with Internal Landmarks could be an effective and practical solution to imaging location which is flexible to prostate volume changes during long-term monitoring and provide an easy-to-understand prostatic mapping allowing the operators to be fully aware of the orientation and anatomical origin of the tissues (Fig. 13–15, 19).

4.2.2. Characteristic Internal landmarks (the second question)

In this study, we found out that among the total 1846 Internal Landmarks collected from 164 patients, prostatic calcifications were most commonly utilized (62%) as anchor points to facilitate accurate imaging correlation during the process of Trend Monitoring, then followed by prostatic cysts (28%), seminal colliculus (7%) and others (3%), respectively.

Prostatic calcification is a common finding during TRUS in both healthy subjects and patients. They are rare in children, infrequent below the age of 40, sharply increase in quantity and size over 50 and continue with further aging [42]. In a study of 300 asymptomatic adult men, Søndergaard et al. reported prostatic calcifications in 99% of the cases at the time of autopsy [43]. Prostatic calcifications are believed to arise as a result of inspissated prostatic secretions, with a core surrounded by concentric layers of calcium apatite under inflammatory conditions [44]. Normally, they remain asymptomatic throughout an individual's lifetime; however, progression may cause mechanical obstruction, smooth muscle contraction, voiding symptoms and being somehow related to LUTS, chronic prostatitis or chronic pelvic pain syndrome [45]. Prostatic calcifications typically appear as brightly echogenic foci that may or may not show posterior shadowing under TRUS (Fig. 10b) and are mostly found in the posterior and posterolateral zones or centrally located within the anterior aspect of the prostate [43, 44].

Prostatic cysts are also common structures which are discovered by incidental diagnosis on TRUS in 5–8% of patients [46]. In subjects being investigated for infertility, the prevalence could increase to 20% [47]. Congenital prostatic cystic lesions may arise from either müllerian or Wolffian structures. The etiological factors include inflammation, BPH, ejaculatory duct obstruction, atrophy of the prostate gland, tumor, etc. Galosi et al. suggested that prostatic cysts could be classified into 6 categories, including isolated medial cysts, cysts of the ejaculatory duct, simple or multiple cysts of the parenchyma, complicated infectious or hemorrhagic cysts, cystic tumors and cysts secondary to parasitic disease [46]. The sonographic appearance of simple cysts is generally thin walled, anechoic, showing posterior acoustic enhancement (Fig. 10c).

Seminal colliculus is the rounded eminence of the urethral crest located on the posterior wall of the mid prostatic urethra, which marks the boundary between the membranous and the prostatic segment (Fig. 10a). The prostatic utricle opens into it in the midline and the two ejaculatory ducts orifices can be found on both sides. The clinical significance of this

structure is that during TURP operators usually utilize seminal colliculus as a surgical landmark to locate urethral sphincter and the lower limit of the intervention.

Prostatic calcifications, prostatic cysts, seminal colliculus and other specific intraprostatic findings, whether physiologic or pathologic, are proved feasible to support accurate imaging correlation under TRUS in long-term follow-up. Compared to location method based on artificially implanted fiducial markers (e.g. gold seeds), correlating to Internal Landmarks are costless and time-saving. These natural anchor points, being resistant to prostate motion, could possibly reduce the effect of marker migration and help to avoid complications of fiducial insertion such as pain, fever, voiding complaints, hematuria, hematospermia, rectal bleeding, gold allergy [26].

4.3. Internal Fusion vs. External Fusion

In this study we also proposed the brand-new concepts of “Internal Fusion” and “External Fusion”. Generally, for any targeted imaging methods, three essential parts need to be considered during the biopsy procedure. First, reliably detect the truly tumor-suspicious areas of the prostate. Second, accurately locate the pre-planned targets under real-time imaging (usually US) control to guide the biopsy needle. Third, reliably re-locate the biopsied sites or any other ROI during long-term monitoring of tissue changes. In MRI/US fusion technique, abnormal areas marked on the pre-conducted MRI are mapped or registered onto the real-time US visualization by devices with integrated fusion software so that targeted biopsies could be performed. This combination of two different imaging modalities naturally generates the term “External Fusion”. Meanwhile, ANNA/C-TRUS detects non-visual lesions simply by analyzing US images with pathology-based AI algorithm and locate the targets by correlating to intraprostatic landmarks (Internal Landmarks), so that this single-imaging-modality-based technique was termed as “Internal Fusion”.

Though mpMRI could objectively provide more image information than conventional grey-scale US due to the additional functional sequences, there are still several issues worthy

of further consideration in the External Fusion technique. Firstly, the interpretation of MRI is inevitably a subjective procedure carried out by human eyes and brains. Though the Prostate Imaging Reporting and Data System (PI-RADS) was published to standardize the evaluation and reporting of prostate MRI [48], discordance of interpretation results and PI-RADS score assignment still exists even between experts [49–51] and a considerable number of clinically significant lesions could be missed [52, 53]. The followed sophisticated step of MRI/US fusion would be meaningless if the capability and reliability of lesion detection in the very first step were questioned. Secondly, the accuracy of targets registration and fusion between two different imaging modalities is challenged. Reports showed discordance between MRI and TRUS measured prostate volume and prostate displacements may occur during the period between the pre-conducted MRI examination and the final fusion biopsy procedure [51, 54]. Other factors including patient orientation, filling of bladder or rectum, pressure of TRUS probe or endorectal coil, and even the biopsies themselves, may cause local shape deformations of the prostate, which need to be corrected by additional fusion algorithm in real time [33]. To exclude the effect of movements, general anesthesia is commonly accepted in External Fusion biopsy, which demands longer procedure durations, cardiopulmonary risk to the patients and additional cost compared to TRUS biopsy [55, 56]. Besides, cognitive operation is still inevitable when defining the outline of the prostate and selecting the actual needle positions, hence current literatures of comparison between cognitive, direct in-bore or MRI/US fusion guidance do not show a clear superiority of one technique over the others, questioning the value of External Fusion [15, 57, 58].

To overcome these limitations, machine learning tools are explored. Internal Fusion offers an alternative of objective image interpretation and targets localization. By following the SOP of AI-US-CT in the routine clinical practice, we observed a PCa detection rate of 52% with only 5.2 biopsy cores in average, and this rate is even higher (70%) in patients with initial biopsies. Similar results are supported by an undergoing randomized controlled trial (RCT) that ANNA/C-TRUS guided biopsy performed better in PCa detection rate with less biopsy cores than mpMRI assisted biopsy [59]. Correlation to Internal Landmarks ensures re-location and continuous assessment of system archived biopsy sites with pathological grades over time in

high accuracy (94%), depending on local pathological anatomy and operator's experience. Data from a 12-year follow-up in our institution showed that under ANNA/C-TRUS based monitoring, 50–75% of the usually performed biopsy cores could be spared and 97% of the patients were either without evidence of a PCa or were diagnosed in time to be sufficiently treated [23]. These promising results indicate that Trend Monitoring implemented with Internal Fusion technique could possibly offer a new opportunity not only in continuous observation of prostatic natural change or disease progression by imaging as a complement to longitudinal PSA, but also to perform per-lesion-based active surveillance or focal therapy. Being cost-effective and user-friendly, this US-based approach saves the additional equipment and software installation, the complex procedures which need to be fulfilled in separate sessions, and the patients' discomfort associated with magnet bore and coil noise in External Fusion process [60].

4.4. Study limitations and future developments

Firstly, this study included patients who had underwent surgical treatments for BPH including TURP or PAE and patients diagnosed with PCa accepting radiotherapy or hormonal therapy. These treatments could change the anatomical structure and US appearance of the remaining tissues of the prostate as well as the Internal Landmarks. This could possibly explain the difference of imaging correlation rate between in vitro and in vivo (100% vs. 94%) and different subgroups in vivo. Larger number of patients in this subgroup need to be analyzed in future to find out the possible influence factors of correlation rate.

Additionally, most patients included in current study had an age beyond 50. The imaging locating method in younger group who only intended for prostate health inspection, i.e. with few calcifications and cysts (not found in current study yet), need to be further considered.

Finally, the current study is only an observational study carried out in single cohort by single medical center. Multicenter RCTs could be proposed in future to verify the possible positive

meanings and values of Internal Landmarks in assisting active surveillance and focal therapy for PCa.

5. Conclusion

Introduction & objectives

Nowadays innovative imaging modalities are applied for diagnosing and follow-up of prostate cancer (PCa). In order to monitor tissue changes (Trend Monitoring) and perform authentic targeted biopsy, it is essential to reliably identify the same region of interest (ROI) or cross-sections of the prostate and hit targets in their true anatomical locations over time. Transrectal ultrasound (TRUS) identifiable morphologic structures including prostatic calcifications, cysts, asymmetries or anatomical fix-points (e.g. seminal colliculus) are utilized as natural anchor points (Internal Landmarks) to facilitate exact imaging correlation, and this technique is termed as “Internal Fusion”. This observational study analyses the feasibility and accuracy of Internal Landmarks in assistance for Trend Monitoring and targeted biopsy by artificial neural network analysis/computerized TRUS (ANNA/C-TRUS).

Materials & methods

From January 2017 to May 2018, patients with at least one prior series of 5-mm spaced TRUS images analyzed by artificial intelligence algorithm and stored as computed tomographic online data set (AI-US-CT) were included. Two experienced operators collected new TRUS images in one-to-one correlation with each prostate cross-section of the previous examinations based on Internal Landmarks and targeted biopsies were taken if with indication. Informed consent was obtained from all individuals observed in the study.

Results

The total 164 patients had an age ranged 46–89 years (median: 73); the prostate-specific antigen (PSA) value ranged 0.02–48.96 ng/ml (median: 3.75); the prostate volumes ranged 7.72–272 ml (median: 41); the interval between first and latest AI-US-CT session ranged 1–113 (median: 50). 8 patients (5%) had been diagnosed with PCa before this study; 69 men (42%) came for mere prevention or early detection; 87 men (53%) were suspicious of PCa and a third of them (29 men) chose ANNA/C-TRUS guided biopsy, and PCa were detected in

15/29 patients (52%) with average 5.2 cores. In initial and repeat biopsy, PCa detection rate reached 70% and 42%, respectively. Overall, 1846 Internal Landmarks were utilized as anchor points during the process of Trend Monitoring, including prostatic calcifications (1128, 62%), cysts (524, 28%), seminal colliculus (133, 7%) and others (61, 3%). Basing on re-locating of these Internal Landmarks, accurate imaging correlations were attained in 1021 out of 1090 TRUS slices (94%), after years, despite volume changes, even generated on different instruments by different operators. The longest Trend Monitoring with exact image correlation in this study had so far reached 9 years and 5 months.

Summary

Internal Landmarks are of vital importance to exact image correlation in long-term monitoring of the prostate. Trend Monitoring by ANNA/C-TRUS could possibly offer a new opportunity not only in continuous observation of prostatic natural change or disease progression by imaging as a complement to longitudinal PSA, but also to perform per-lesion-based active surveillance or focal therapy. In case of PCa suspicion, Internal Fusion helps targeted biopsies in high accuracy with less biopsy cores.

6. Bibliography

1. Huggins C, Scott WW, Heinen JH. Chemical composition of human semen and of the secretions of the prostate and seminal vesicles. *American Journal of Physiology-Legacy Content*. 1942;136(3):467-73.
2. Prajapati A, Gupta S, Mistry B, Gupta S. Prostate Stem Cells in the Development of Benign Prostate Hyperplasia and Prostate Cancer: Emerging Role and Concepts. *BioMed Research International*. 2013;2013:10.
3. Wong MCS, Goggins WB, Wang HHX, Fung FDH, Leung C, Wong SYS, et al. Global Incidence and Mortality for Prostate Cancer: Analysis of Temporal Patterns and Trends in 36 Countries. *European Urology*. 2016;70(5):862-74.
4. Jacques F, Isabelle S, Rajesh D, Sultan E, Colin M, Marise R, et al. Cancer incidence and mortality worldwide: Sources, methods and major patterns in GLOBOCAN 2012. *International Journal of Cancer*. 2015;136(5):E359-E86.
5. Haas GP, Delongchamps N, Brawley OW, Wang CY, de la Roza G. The Worldwide Epidemiology of Prostate Cancer: Perspectives from Autopsy Studies. *The Canadian journal of urology*. 2008;15(1):3866-71.
6. Mottet N, Bellmunt J, Bolla M, Briers E, Cumberbatch MG, De Santis M, et al. EAU-ESTRO-SIOG Guidelines on Prostate Cancer. Part 1: Screening, Diagnosis, and Local Treatment with Curative Intent. *European Urology*. 2017;71(4):618-29.
7. Botchorishvili G, Matikainen MP, Lilja H. Early prostate-specific antigen changes and the diagnosis and prognosis of prostate cancer. *Current opinion in urology*. 2009;19(3):221-6.
8. Catalona WJ, Richie JP, Ahmann FR, Hudson MLA, Scardino PT, Flanigan RC, et al. Comparison of Digital Rectal Examination and Serum Prostate Specific Antigen in the Early Detection of Prostate Cancer: Results of a Multicenter Clinical Trial of 6,630 Men. *The Journal of Urology*. 1994;151(5):1283-90.
9. Bjurlin MA, Carter HB, Schellhammer P, Cookson MS, Gomella LG, Troyer D, et al. Optimization of initial prostate biopsy in clinical practice: sampling, labeling and specimen processing. *The Journal of urology*. 2013;189(6):2039-46.

-
10. Xue J, Qin Z, Cai H, Zhang C, Li X, Xu W, et al. Comparison between transrectal and transperineal prostate biopsy for detection of prostate cancer: a meta-analysis and trial sequential analysis. *Oncotarget*. 2017;8(14):23322-36.
 11. Haas GP, Delongchamps NB, Jones RF, Chandan V, Serio AM, Vickers AJ, et al. Needle Biopsies on Autopsy Prostates: Sensitivity of Cancer Detection Based on True Prevalence. *JNCI: Journal of the National Cancer Institute*. 2007;99(19):1484-9.
 12. Terris MK, McNeal JE, Stamey TA. Detection of Clinically Significant Prostate Cancer by Transrectal Ultrasound-Guided Systematic Biopsies. *The Journal of Urology*. 1992;148(3, Part 1):829-32.
 13. Taira AV, Merrick GS, Galbreath RW, Andreini H, Taubenslag W, Curtis R, et al. Performance of transperineal template-guided mapping biopsy in detecting prostate cancer in the initial and repeat biopsy setting. *Prostate Cancer and Prostatic Diseases*. 2010;13(1):71-7.
 14. Singh H, Canto EI, Shariat SF, Kadmon DOV, Miles BJ, Wheeler TM, et al. Predictors of Prostate Cancer After Initial Negative Systematic 12 Core Biopsy. *The Journal of Urology*. 2004;171(5):1850-4.
 15. Wegelin O, van Melick HHE, Hooft L, Bosch JLHR, Reitsma HB, Barentsz JO, et al. Comparing Three Different Techniques for Magnetic Resonance Imaging-targeted Prostate Biopsies: A Systematic Review of In-bore versus Magnetic Resonance Imaging-transrectal Ultrasound fusion versus Cognitive Registration. Is There a Preferred Technique? *European Urology*. 2017;71(4):517-31.
 16. Simmons L.A., Autier P., Zat'ura F.. Detection, localisation and characterisation of prostate cancer by prostate HistoScanning™. *BJU Int*. 2012; 110(1): 28–35.
 17. Postema A., Idzenga T., Mischi M., Frinking P., de la Rosette J.J., Wijkstra H. Ultrasound modalities and quantification: developments of multiparametric ultrasonography, a new modality to detect, localize and target prostatic tumors. *Curr Opin Urol*. 2015; 25(3): 191–197.
 18. Good D.W., Stewart G.D., Hammer S.. Elasticity as a biomarker for prostate cancer: a systematic review. *BJU Int*. 2014; 113(4): 523–534.

-
19. Loch T, Carey B, Walz J, Fulgham PF. EAU Standardised Medical Terminology for Urologic Imaging: A Taxonomic Approach. *European Urology*. 2015;67(5):965-71.
 20. Loch T, Leuschner I, Genberg C, Weichert-Jacobsen K, Küppers F, Yfantis E, et al. Artificial neural network analysis (ANNA) of prostatic transrectal ultrasound. *The Prostate*. 1999;39(3):198-204.
 21. Loch T. Computerized transrectal ultrasound (C-TRUS) of the prostate: detection of cancer in patients with multiple negative systematic random biopsies. *World Journal of Urology*. 2007;25(4):375-80.
 22. Enzmann T, Tokas T, Korte K, Ritter M, Hammerer P, Franzaring L, et al. Prostatabiopsie. *Der Urologe*. 2015;54(12):1811-22.
 23. Tokas T, Grabski B, Paul U, Bäurle L, Loch T. A 12-year follow-up of ANNA/C-TRUS image-targeted biopsies in patients suspicious for prostate cancer. *World Journal of Urology*. 2018;36(5):699-704.
 24. Xie Y, Tokas T, Grabski B, Loch T. Internal Fusion: exact correlation of transrectal ultrasound images of the prostate by detailed landmarks over time for targeted biopsies or follow-up. *World Journal of Urology*. 2018;36(5):693-8.
 25. Klotz L, Zhang L, Lam A, Nam R, Mamedov A, Loblaw A. Clinical Results of Long-Term Follow-Up of a Large, Active Surveillance Cohort With Localized Prostate Cancer. *Journal of Clinical Oncology*. 2010;28(1):126-31.
 26. Michael N, Elizabeth B, Andrew W, Michael C, Nathan L, Raphael C. Fiducial markers and spacers in prostate radiotherapy: current applications. *BJU International*. 2014;113(S2):13-20.
 27. Loch AC, Bannowsky A, Baeurle L, Grabski B, König B, Flier G, et al. Technical and anatomical essentials for transrectal ultrasound of the prostate. *World Journal of Urology*. 2007;25(4):361-6.
 28. McNeal JE, Redwine EA, Freiha FS, Stamey TA. Zonal distribution of prostatic adenocarcinoma. Correlation with histologic pattern and direction of spread. *Am J Surg Pathol*. 1988;12(12):897-906.
 29. Terris MK, Stamey TA. Determination of Prostate Volume by Transrectal Ultrasound. *The Journal of Urology*. 1991;145(5):984-7.

-
30. Stamey TA, Freiha FS, McNeal JE, Redwine EA, Whittemore AS, Schmid HP. Localized prostate cancer. Relationship of tumor volume to clinical significance for treatment of prostate cancer. *Cancer*. 1993;71(S3):933-8.
 31. Ploussard G, Epstein JI, Montironi R, Carroll PR, Wirth M, Grimm M-O, et al. The Contemporary Concept of Significant Versus Insignificant Prostate Cancer. *European Urology*. 2011;60(2):291-303.
 32. Ukimura O, Faber K, Gill IS. Intraprostatic targeting. *Current Opinion in Urology*. 2012;22(2).
 33. Verma S, Choyke PL, Eberhardt SC, Oto A, Tempany CM, Turkbey B, et al. The Current State of MR Imaging-targeted Biopsy Techniques for Detection of Prostate Cancer. *Radiology*. 2017;285(2):343-56.
 34. McNeal JE, Redwine EA, Freiha FS, Stamey TA. Zonal Distribution of Prostatic Adenocarcinoma: Correlation with Histologic Pattern and Direction of Spread. *Am J Surg Pathol*. 1988;12(12).
 35. El-Hakim A, Moussa S. CUA guidelines on prostate biopsy methodology. *Can Urol Assoc J*. 2010;4(2):89-94.
 36. Abdulmajed MI, Hughes D, Shergill IS. The role of transperineal template biopsies of the prostate in the diagnosis of prostate cancer: a review. *Expert Review of Medical Devices*. 2015;12(2):175-82.
 37. Rhodes T, Girman Cynthia J, Jacobsen Steven J, Roberts Rosebud O, Guess Harry A, Lieber Michael M. Longitudinal prostate growth rates during 5 years in randomly selected community men 40 to 79 years old. *Journal of Urology*. 1999;161(4):1174-9.
 38. McConnell JD. Medical management of benign prostatic hyperplasia with androgen suppression. *The Prostate*. 1990;17(S3):49-59.
 39. McConnell JD, Bruskewitz R, Walsh P, Andriole G, Lieber M, Holtgrewe HL, et al. The Effect of Finasteride on the Risk of Acute Urinary Retention and the Need for Surgical Treatment among Men with Benign Prostatic Hyperplasia. *New England Journal of Medicine*. 1998;338(9):557-63.

-
40. Stone Nelson N, Stock Richard G. The Effect of Brachytherapy, External Beam Irradiation and Hormonal Therapy on Prostate Volume. *Journal of Urology*. 2007;177(3):925-8.
 41. Whittington R, Broderick GA, Arger P, Malkowicz SB, Epperson RD, Arjomandy B, et al. The effect of androgen deprivation on the early changes in prostate volume following transperineal ultrasound guided interstitial therapy for localized carcinoma of the prostate. *International Journal of Radiation Oncology • Biology • Physics*. 1999;44(5):1107-10.
 42. Klimas R, Bennett B, Gardner Jr WA. Prostatic calculi: A review. *The Prostate*. 1985;7(1):91-6.
 43. SØndergaard G, Vetner MAX, Christensen PO. Prostatic Calculi. *Acta Pathologica Microbiologica Scandinavica Series A :Pathology*. 1987;95A(1 - 6):141-5.
 44. Hyun JS. Clinical Significance of Prostatic Calculi: A Review. *World J Mens Health*. 2018;36(1):15-21.
 45. Geramoutsos I, Gyftopoulos K, Perimenis P, Thanou V, Liagka D, Siambli D, et al. Clinical Correlation of Prostatic Lithiasis with Chronic Pelvic Pain Syndromes in Young Adults. *European Urology*. 2004;45(3):333-8.
 46. Galosi Andrea B, Montironi R, Fabiani A, Lacetera V, Gallé G, Muzzonigro G. Cystic Lesions of the Prostate Gland: An Ultrasound Classification With Pathological Correlation. *Journal of Urology*. 2009;181(2):647-57.
 47. Kim ED, Onel E, Honig SC, Lipshultz LI. The prevalence of cystic abnormalities of the prostate involving the ejaculatory ducts as detected by transrectal ultrasound. *International Urology and Nephrology*. 1997;29(6):647-52.
 48. Hamoen EHJ, de Rooij M, Witjes JA, Barentsz JO, Rovers MM. Use of the Prostate Imaging Reporting and Data System (PI-RADS) for Prostate Cancer Detection with Multiparametric Magnetic Resonance Imaging: A Diagnostic Meta-analysis. *European Urology*. 2015;67(6):1112-21.
 49. Müller S, Lilleaasen G, Sand TE, Løfsgaard L, Estop-Garanto M, Helgø D, et al. Poor reproducibility of PIRADS score in two multiparametric MRIs before biopsy in men with elevated PSA. *World journal of urology*. 2018;36(5):687-91.

-
50. Sonn GA, Fan RE, Ghanouni P, Wang NN, Brooks JD, Loening AM, et al. Prostate Magnetic Resonance Imaging Interpretation Varies Substantially Across Radiologists. *European Urology Focus*. 2019;5(4):592-9.
 51. Cash H, Günzel K, Maxeiner A, Stephan C, Fischer T, Durmus T, et al. Prostate cancer detection on transrectal ultrasonography-guided random biopsy despite negative real-time magnetic resonance imaging/ultrasonography fusion-guided targeted biopsy: reasons for targeted biopsy failure. *BJU International*. 2016;118(1):35-43.
 52. Borofsky S, George AK, Gaur S, Bernardo M, Greer MD, Mertan FV, et al. What Are We Missing? False-Negative Cancers at Multiparametric MR Imaging of the Prostate. *Radiology*. 2018;286(1):186-95.
 53. Johnson DC, Raman SS, Mirak SA, Kwan L, Bajgiran AM, Hsu W, et al. Detection of Individual Prostate Cancer Foci via Multiparametric Magnetic Resonance Imaging. *European Urology*. 2019;75(5):712-20.
 54. Christie DRH, Sharpley CF. How Accurately Can Prostate Gland Imaging Measure the Prostate Gland Volume? Results of a Systematic Review. *Prostate Cancer*. 2019;2019:6932572-.
 55. Kuru Timur H, Roethke Matthias C, Seidenader J, Simpfendörfer T, Boxler S, Alammar K, et al. Critical Evaluation of Magnetic Resonance Imaging Targeted, Transrectal Ultrasound Guided Transperineal Fusion Biopsy for Detection of Prostate Cancer. *Journal of Urology*. 2013;190(4):1380-6.
 56. Kuru TH, Saeb-Parsy K, Cantiani A, Frey J, Lombardo R, Serrao E, et al. Evolution of repeat prostate biopsy strategies incorporating transperineal and MRI–TRUS fusion techniques. *World Journal of Urology*. 2014;32(4):945-50.
 57. Puech P, Rouvière O, Renard-Penna R, Villers A, Devos P, Colombel M, et al. Prostate Cancer Diagnosis: Multiparametric MR-targeted Biopsy with Cognitive and Transrectal US–MR Fusion Guidance versus Systematic Biopsy—Prospective Multicenter Study. *Radiology*. 2013;268(2):461-9.
 58. Arsov C, Rabenalt R, Blondin D, Quentin M, Hiester A, Godehardt E, et al. Prospective Randomized Trial Comparing Magnetic Resonance Imaging (MRI)-guided In-bore Biopsy

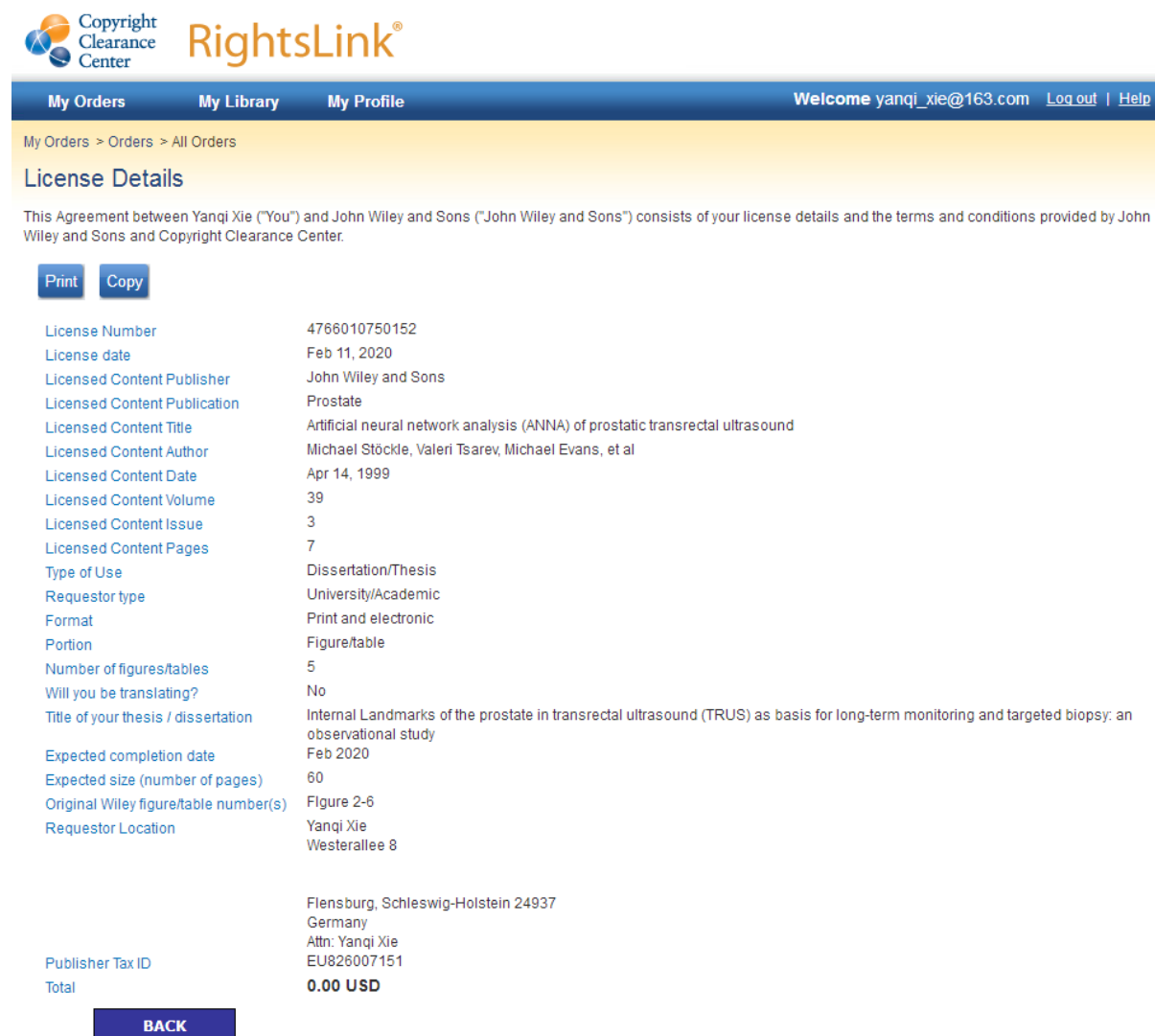
- to MRI-ultrasound Fusion and Transrectal Ultrasound-guided Prostate Biopsy in Patients with Prior Negative Biopsies. *European Urology*. 2015;68(4):713-20.
59. Xie LP, Wang X, Zheng XY, Liu B, Li JF, Wang S. 500 - A randomized controlled trial to assess and compare the outcomes of AI-US-CT guided biopsy, transrectal ultrasound guided 12-core systematic biopsy, and mpMRI assisted 12-core systematic biopsy. *European Urology Supplements*. 2017;16(3):e865-e6.
60. Quirk ME, Letendre AJ, Ciottone RA, Lingley JF. Anxiety in patients undergoing MR imaging. *Radiology*. 1989;170(2):463-6.

7. Appendices

7.1. Figure and table index

Fig. 1 Depiction of ANNA/C-TRUS	4
Fig. 2 Diagram of the artificial neural network used for ANNA	5
Fig. 3 TRUS image of fiducial markers	6
Fig. 4 Ultrasound prostate phantom	9
Fig. 5 Validation of Internal Landmarks in vivo	10
Fig. 6 Validation of Internal Landmarks in single AI-US-CT session	12
Fig. 7 Water balloon standoff on US transducer	14
Fig. 8 A “survey” scan of the prostate	16
Fig. 9 Volume measurement of the prostate	17
Fig. 10 TRUS images correlation in Trend Monitoring	19
Fig. 11 Depiction of AI-US-CT	21
Fig. 12 Biopsy gun and biopsy samples	22
Fig. 13 ANNA results changes in follow-up	23
Fig. 14 Internal Fusion	24
Fig. 15 Documentation of biopsy data	25
Fig. 16 Internal Landmarks in vivo	28
Fig. 17 Distribution Characteristics of patients under Trend Monitoring	29
Fig. 18 Re-locating of the same cross-sections by Internal Landmarks over time	34
Fig. 19 Long-term Trend Monitoring with accurate image correlation	35
Table 1 Landmarks validation in vitro	27
Table 2 Patient demographics	32
Table 3 Characteristics of correlated Internal Landmarks and TRUS images in follow-up ...	36
Table 4 Characteristics of targeted biopsies	38

7.2. Permissions of reusing published figures



Copyright Clearance Center **RightsLink®**

My Orders My Library My Profile Welcome yanqi_xie@163.com [Log out](#) | [Help](#)

My Orders > Orders > All Orders

License Details

This Agreement between Yanqi Xie ("You") and John Wiley and Sons ("John Wiley and Sons") consists of your license details and the terms and conditions provided by John Wiley and Sons and Copyright Clearance Center.

[Print](#) [Copy](#)

License Number	4766010750152
License date	Feb 11, 2020
Licensed Content Publisher	John Wiley and Sons
Licensed Content Publication	Prostate
Licensed Content Title	Artificial neural network analysis (ANNA) of prostatic transrectal ultrasound
Licensed Content Author	Michael Stöckle, Valeri Tsarev, Michael Evans, et al
Licensed Content Date	Apr 14, 1999
Licensed Content Volume	39
Licensed Content Issue	3
Licensed Content Pages	7
Type of Use	Dissertation/Thesis
Requestor type	University/Academic
Format	Print and electronic
Portion	Figure/table
Number of figures/tables	5
Will you be translating?	No
Title of your thesis / dissertation	Internal Landmarks of the prostate in transrectal ultrasound (TRUS) as basis for long-term monitoring and targeted biopsy: an observational study
Expected completion date	Feb 2020
Expected size (number of pages)	60
Original Wiley figure/table number(s)	Figure 2-6
Requestor Location	Yanqi Xie Westerallee 8 Flensburg, Schleswig-Holstein 24937 Germany Attn: Yanqi Xie EU826007151
Publisher Tax ID	
Total	0.00 USD

[BACK](#)

Copyright © 2020 Copyright Clearance Center, Inc. All Rights Reserved. [Privacy statement](#) . [Terms and Conditions](#) . [Comments?](#) We would like to hear from you. E-mail us at customercare@copyright.com

7.3. Publications

1. Xie Y, Tokas T, Grabski B, Loch T. Internal Fusion: exact correlation of transrectal ultrasound images of the prostate by detailed landmarks over time for targeted biopsies or follow-up. *World Journal of Urology*. 2018;36(5):693-8.

2. 3. Vortragspreis-klinisch in 72. Kongress der Deutschen Gesellschaft für Urologie e.V.:
Trend Monitoring (TM) and targeted biopsy by artificial intelligence ultrasound of the
prostate (AIUSP).

8. Acknowledgements

First of all, I would like to express my sincere gratitude to my supervisor, Prof. Dr. med. Tillmann Loch, for offering me the chance of working and studying in this project. I am deeply grateful to his guidance for the publication and the dissertation, including sharing the original idea, manuscript editing, and all the other supports concerning my doctoral work. I would also like to thank for the care from him and his family during my stay in Germany.

I would like to express my sincere appreciation to Prof. Dr. Klaus-Peter Jünemann, for his great support and co-supervision of my dissertation.

I would like to thank Dr. med. Patrick Berg, for the patience of sharing his experience of the doctoral degree procedure and the great help for the printing and submission of my work.

I would like to thank Dr. Björn Grabski, for his help in the clinical practice and the precious friendship.

I would like to thank Dr. Theodoros Tokas, for his help in manuscript editing of the published article.

I would like to thank Dr. med. Azizbek Ramankulov, Dr. Andreas Probst, Ms. Hannelene Gersen and other colleagues in the urological department of Diakonissen Hospital Flensburg, and Ms. Jannika Gersen, Mr. Gert Kotter, Mr. Bernd Müller, Ms. Heidi Engemann, Ms. Tian Hao, Ms. Lili Zhou for their kindness and help.

I would like to thank all the patients in this study, for their consent and cooperation.

Last but not least, I would like to thank my family for the constant support and encouragement for my study and life.

9. Curriculum Vitae

Personal data

Family name: Xie

First name: Yanqi

Gender: Male

Date of birth: 22.05.1990

Birthplace: Hangzhou, Zhejiang

Nationality: Chinese

Education

09.1996-07.2002 Hangzhou Tianchang Primary School

09.2002-07.2005 Hangzhou Qingchun Middle School

09.2005-07.2008 Hangzhou No.2 High School of Zhejiang Province

09.2008-07.2013 Hebei Medical University (Clinical Medicine, Bachelor's Degree)

09.2013-06.2016 Tongji Medical College, Huazhong University of Science and Technology
(Urology, Surgery, Master's Degree)

11.2016-09.2018 research project to acquire the doctoral degree (Dr. med.) in
Diakonissenkrankenhaus Flensburg, Akademisches Lehrkrankenhaus der
Christian-Albrechts-Universität zu Kiel

10.2018-09.2021 standardized training of residents in the Second Affiliated Hospital of
Zhejiang University School of Medicine